

**Northwestern Polytechnical University
Statement of originality of the dissertation**

西北工业大学
学位论文原创性声明

秉承学校严谨的学风和优良的科学道德，本人郑重声明：所呈交的学位论文，是本人在导师的指导下进行研究工作所取得的成果。尽我所知，除文中已经注明引用的内容和致谢的地方外，本论文不包含任何其他个人或集体已经公开发表或撰写过的研究成果，不包含本人或其他已申请学位或其他用途使用过的成果。对本文的研究做出重要贡献的个人和集体，均已在文中以明确方式表明。

本人学位论文与资料若有不实，愿意承担一切相关的法律责任。

Design and Control for Reusable Booster of Launch Vehicle

BY

SIMON LE BERRE

UNDER THE SUPERVISION OF PROFESSOR

GONG CHUNLIN

MASTER OF FLIGHT VEHICLE DESIGN

XI'AN P. R. CHINA

JUNE 2020



Design and Control for Reusable Booster of Launch Vehicle

How improve the re-entry of the launch vehicle ?



Summary

- Improvement RLV shape design
- Trajectory design and simulation
- End phase control design
- Validation of end phase control



Summary

- Improvement RLV shape design
 - Validation process
 - Using of flight control
 - Selected model
 - Result of tests
 - Idea of general shape review
- Trajectory design and simulation
- End phase control design
- Validation of end phase control

- Validation process

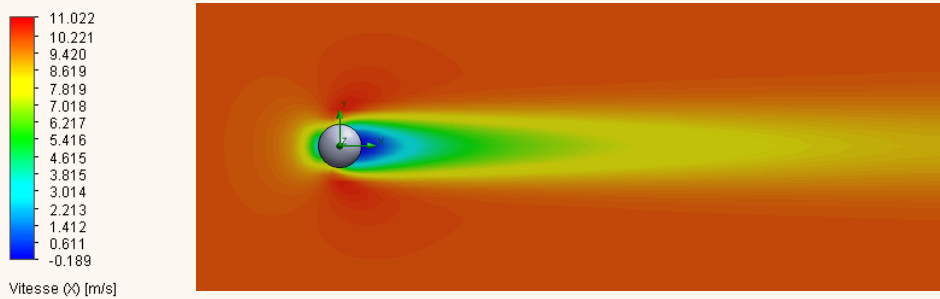
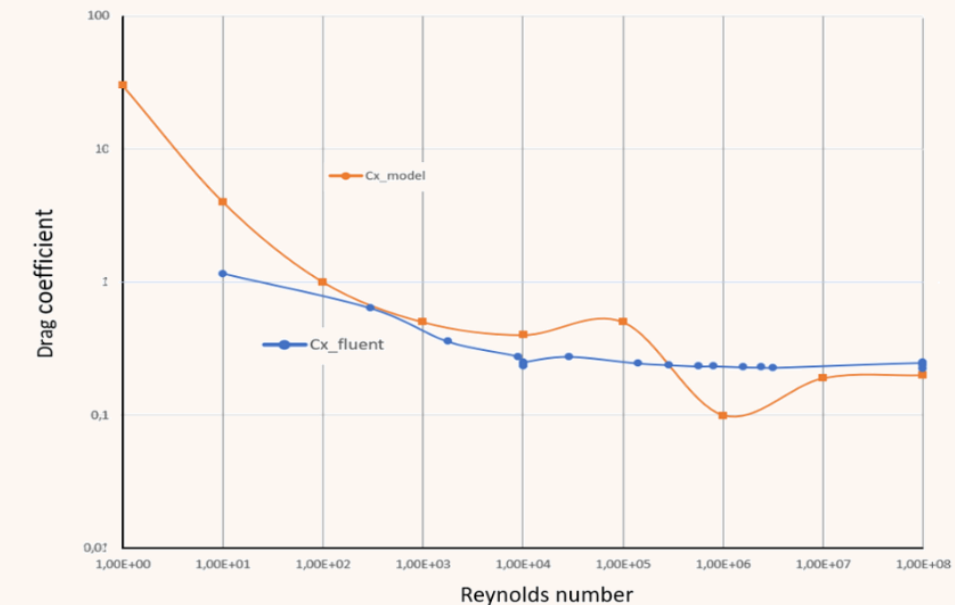


Fig. 1. Representation of the drag of a sphere in a velocity field



*Fig. 2. Drag coefficient function of Reynold number:
- Theoretical curve
- Experimental curve*

- Using of flight control



Fig. 3. Russian missile equipped with grid fin for controller

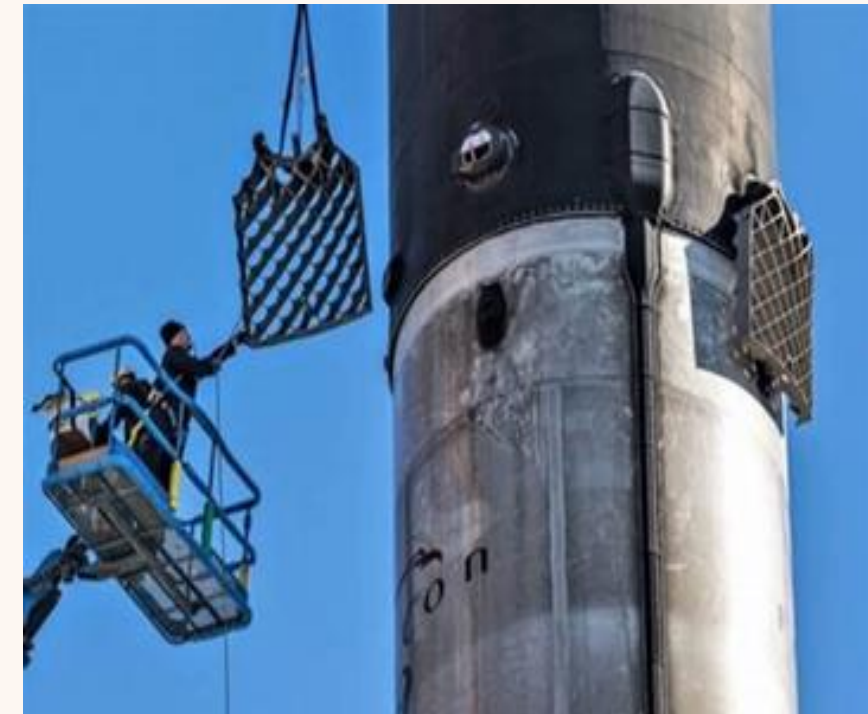


Fig. 4. Falcon 9 booster during the assembly of the Grid fins

- Using of flight control

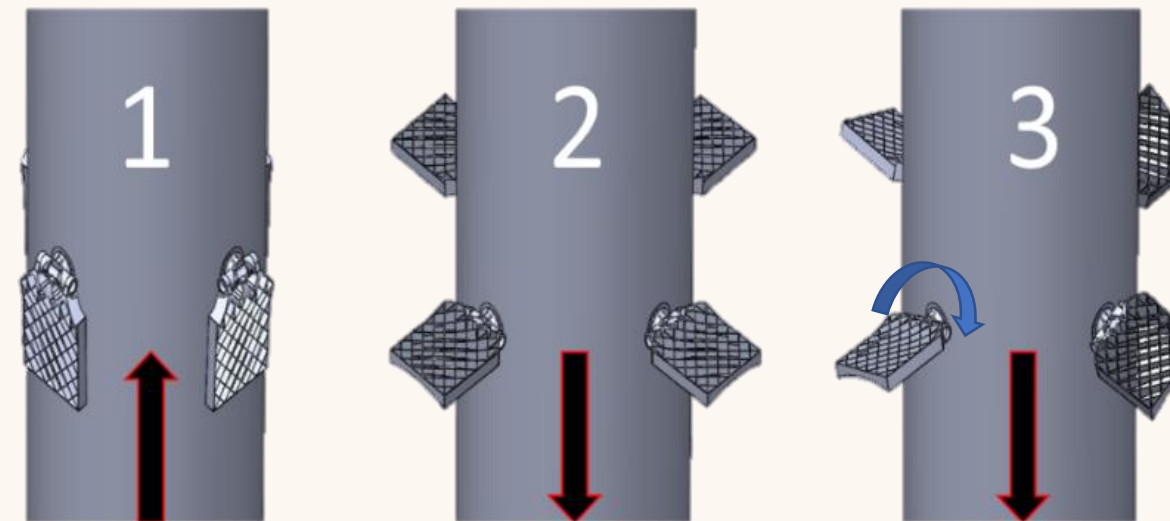


Fig. 5. Using of Grid fins



- Selected model

Validation requirement:

1. Drag force
2. Lift/control force : linearity
3. Drag force during the take-off phase
4. Maximum temperature
5. Weight
6. Size
7. Cost

Fixed parameters:

1. Material : Titan Ti-6242 (using by SpaceX for Grid fins)
2. Size : $S_0 = 1.427 \text{ m}^2$
3. Speed : $V = 1650 \text{ m.s}^{-1}$

- Selected model

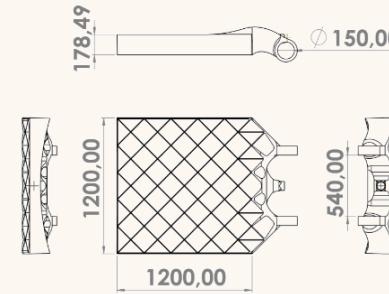
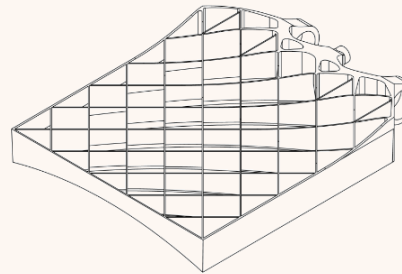


Fig. 6. SpaceX « Gird fin »

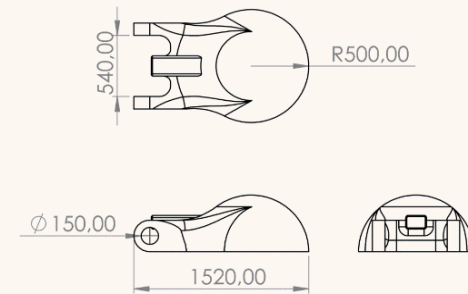
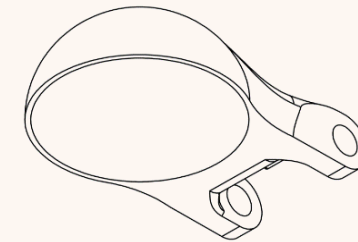


Fig. 7. Model « Bell Brake »

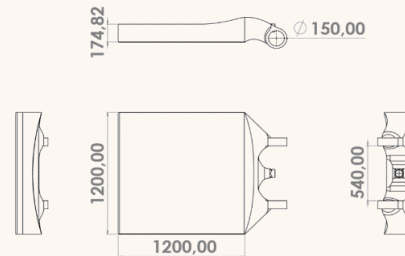
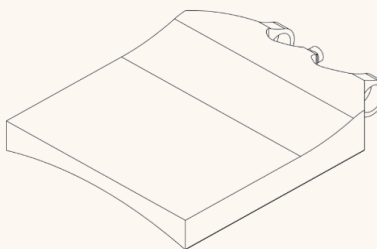


Fig. 8. Model « Flat Fin »

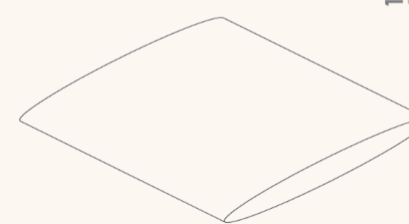


Fig. 9. Model « Simple fin »

- Result of tests

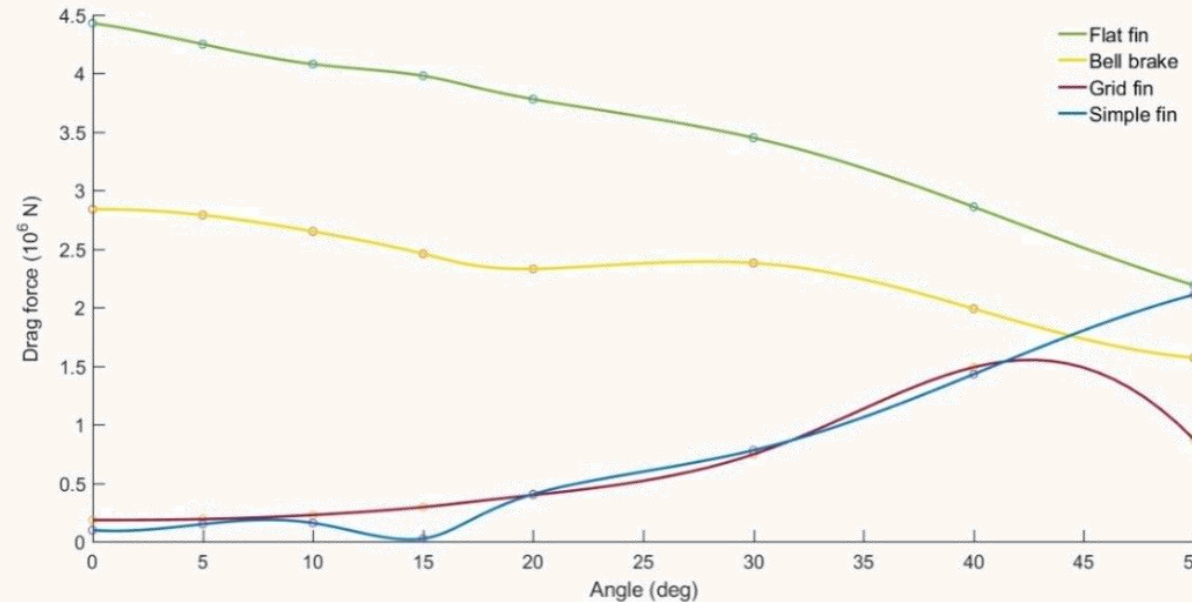
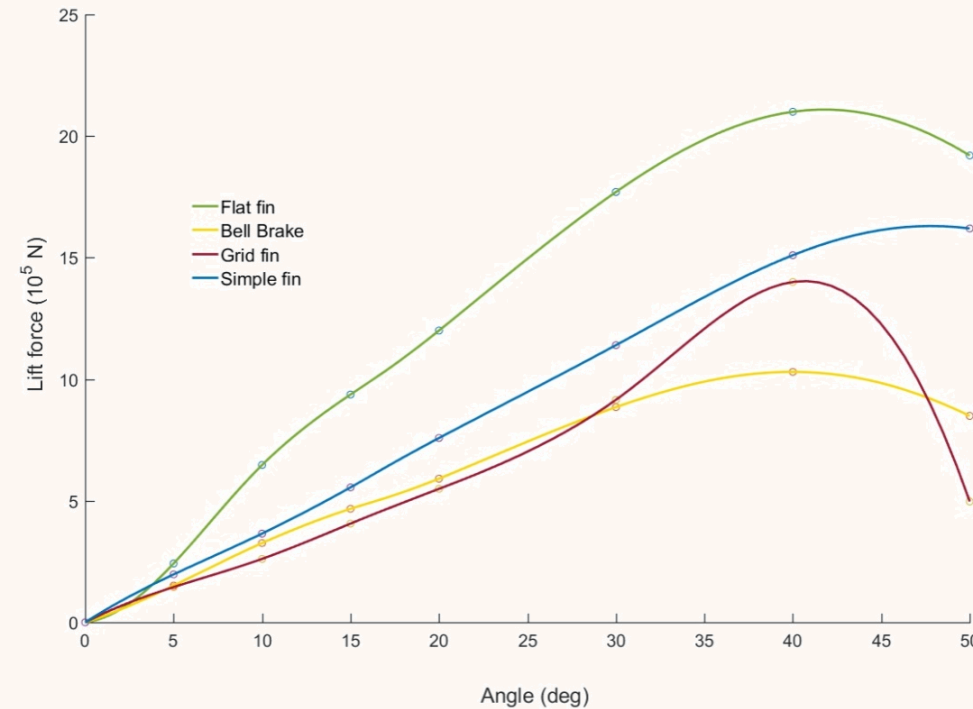


Fig. 10. Drag force function of the angle of correction

Remark: Mathematic point N°1

- Result of tests



$$\text{Lift. force}(angle) = 3.5468 \cdot 10^4 * angle$$

Fig. 11. Lift force function of the angle of correction

Note: Lift force = Correction force

- Result of tests

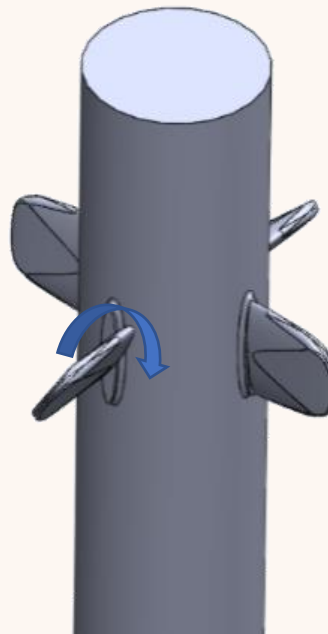


Fig. 12. RLV 3D model using the « Simple Fins »

- Idea of general shape review

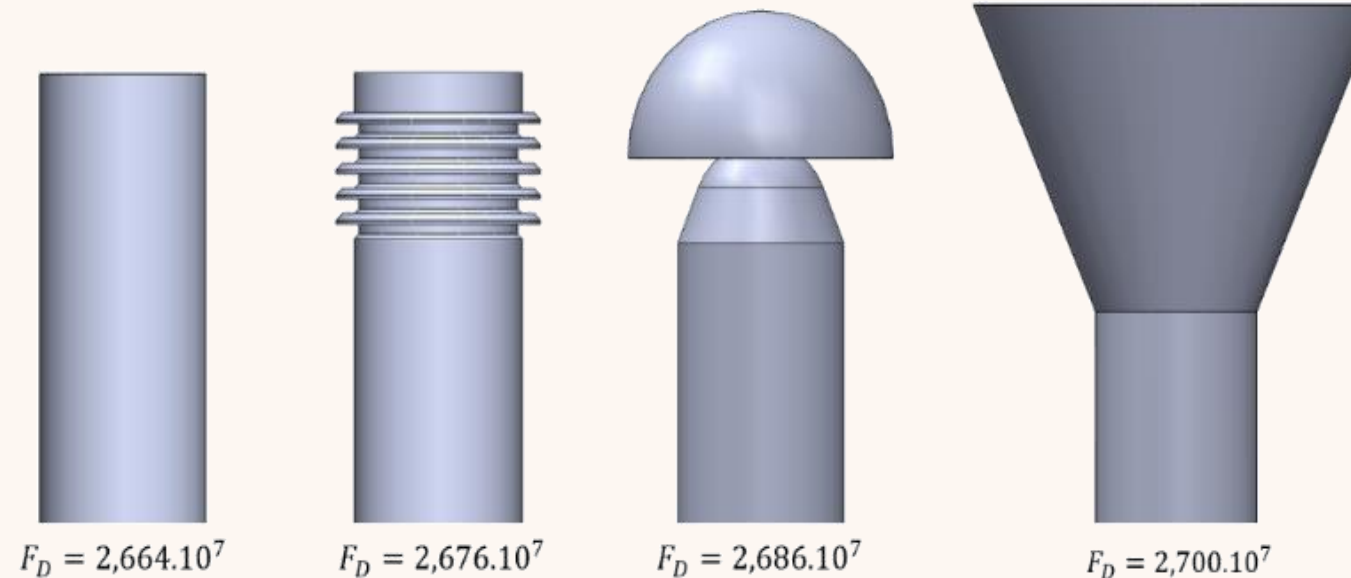


Fig. 13. Some RLV tops with their associated drag force

- Idea of general shape review

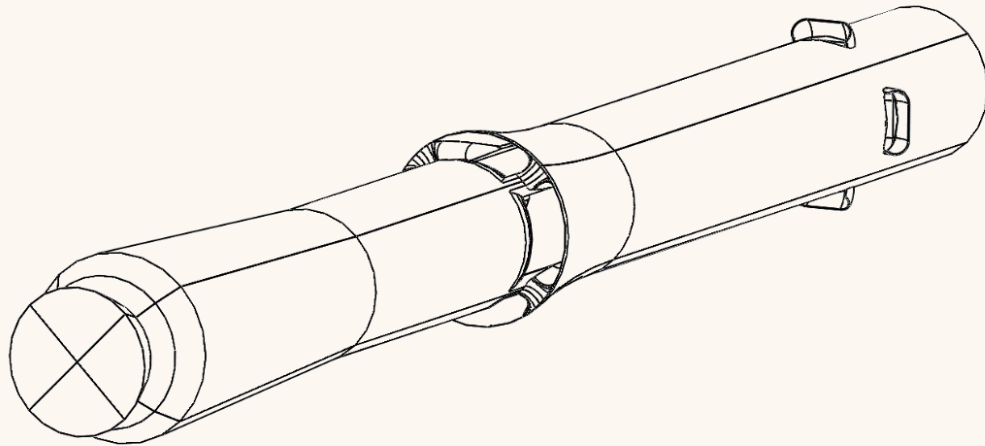


Fig. 14. Model overview

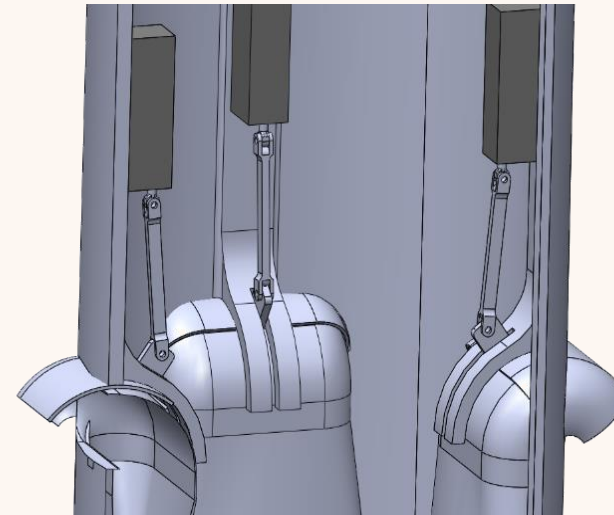


Fig. 15. Controller elbows

- Idea of general shape review

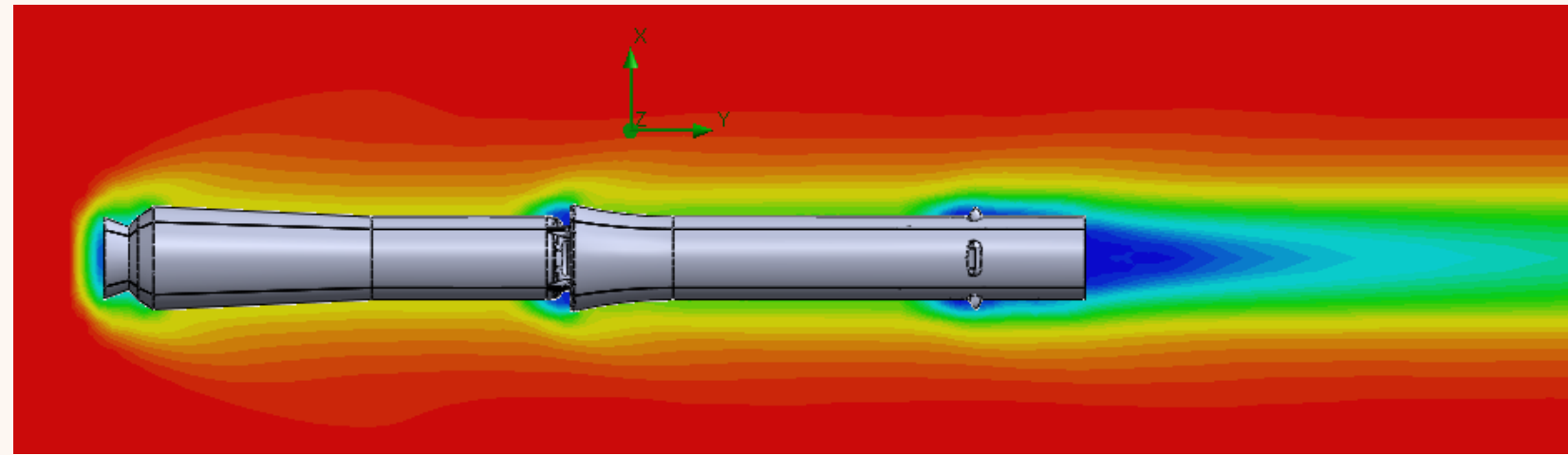


Fig. 16. Representation of the model in an air flow



Summary

- Improvement RLV shape design
- Trajectory design and simulation
- End phase control design
- Validation of end phase control



Summary

- Improvement RLV shape design
- Trajectory design and simulation
 - Presentation and equation of model
 - Aerodynamic tests
 - MATLAB model
 - Simulations and results
- End phase control design
- Validation of end phase control

- Presentation and equation of model

$$m \cdot \ddot{x} = -D \cdot \sin(\theta - \alpha) + L \cdot \cos(\theta - \alpha) + F_c \cdot \cos(\theta) \quad (5)$$

$$m \cdot \ddot{y} = -g + D \cdot \cos(\theta - \alpha) + L \cdot \sin(\theta - \alpha) + F_c \cdot \sin(\theta) \quad (6)$$

$$I \cdot \ddot{\theta} = \frac{L_{RLV}}{1.83} \cdot F_c \quad (7)$$

$$D = q(y) \cdot S \cdot C_D(\alpha, V) \quad (8)$$

$$L = q(y) \cdot S \cdot C_L(\alpha, V) \quad (9)$$

$$q(y) = \frac{1}{2} \cdot \rho(y) \cdot V^2 \quad (10)$$

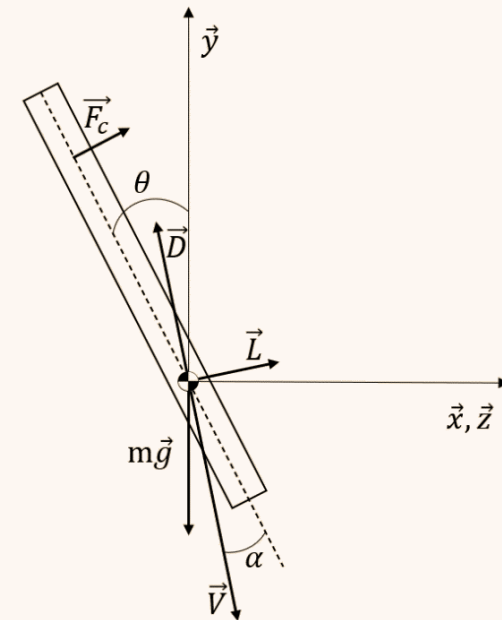


Fig. 17. Physical model of the launcher during the atmospheric re-entry phase

- Presentation and equation of model

Marcel DELEZE, «Atmospheric density as a function of altitude according to the barometric levelling model»

$$\rho(y) = \frac{M p(y)}{R T(y)} = \frac{M}{R} \frac{p_0}{T_0 - a.y} \left(1 - \frac{a}{T_0} y\right)^{\frac{Mg}{Ra}} \quad (11)$$

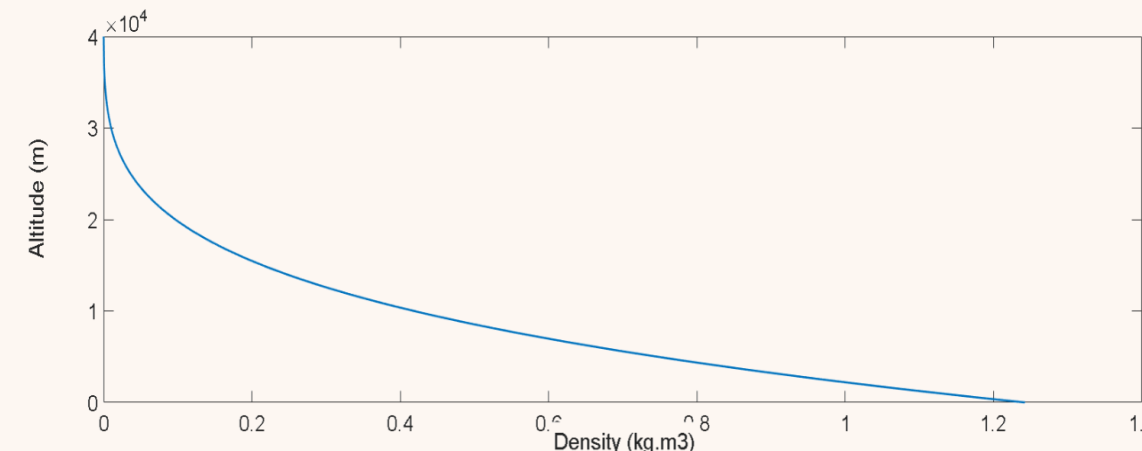


Fig. 18. Density function of the altitude

- Aerodynamic tests

$$C_D(\alpha, V) \quad C_L(\alpha, V)$$

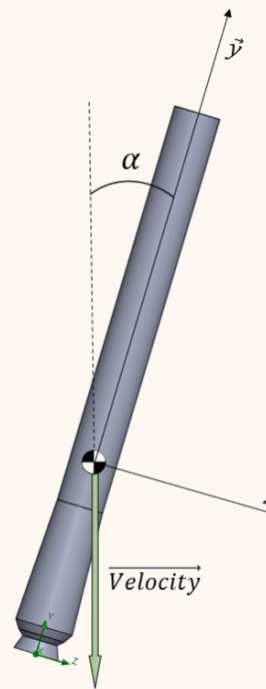


Fig. 19. Test model

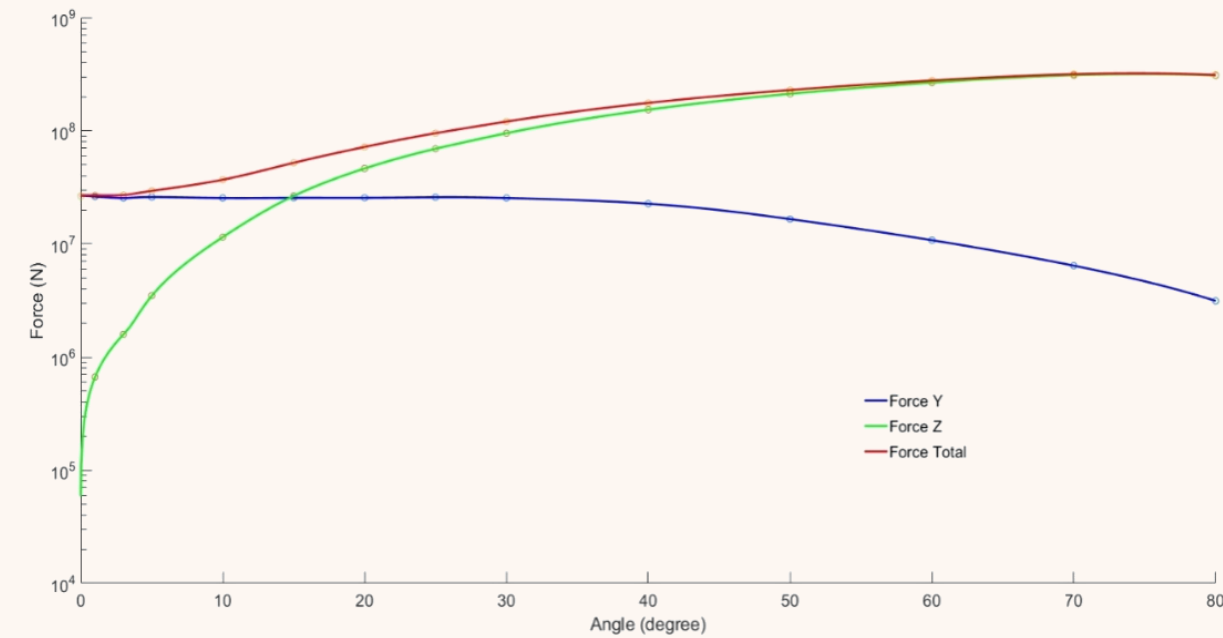


Fig. 20. Y-Force and Z-Force as a function of the angle of attack

- Aerodynamic tests

$$C_D(\alpha, V) \quad C_L(\alpha, V)$$

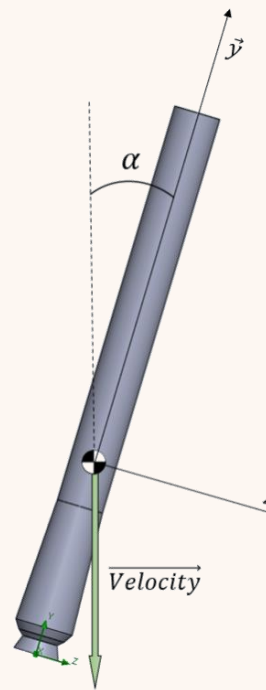


Fig. 19. Test model

Tab. 1. Aerodynamic force ratio

Angle	Force y	Force z	Drag force	Ratio/drag_force_0	Lift force	Ratio/Drag_force
0	2,65E+07	0,00E+00	2,65E+07	1	0,00E+00	0
1	2,63E+07	6,68E+05	2,63E+07	0,993	2,09E+05	0,008
3	2,55E+07	1,59E+06	2,55E+07	0,964	2,54E+05	0,010
5	2,60E+07	3,49E+06	2,62E+07	0,989	1,22E+06	0,047
10	2,55E+07	1,15E+07	2,71E+07	1,024	6,91E+06	0,255
15	2,56E+07	2,66E+07	3,16E+07	1,192	1,91E+07	0,605
20	2,56E+07	4,65E+07	4,00E+07	1,510	3,49E+07	0,873
25	2,59E+07	6,95E+07	5,28E+07	1,996	5,20E+07	0,985
30	2,55E+07	9,54E+07	6,97E+07	2,634	6,99E+07	1,002
40	2,27E+07	1,54E+08	1,17E+08	4,403	1,04E+08	0,888
50	1,66E+07	2,13E+08	1,74E+08	6,579	1,24E+08	0,715
60	1,08E+07	2,68E+08	2,38E+08	8,973	1,25E+08	0,525
70	6,43E+06	3,11E+08	2,94E+08	11,113	1,00E+08	0,341
80	3,14E+06	3,09E+08	3,05E+08	11,532	5,07E+07	0,166



- Aerodynamic tests

$$C_D(\alpha, V) \quad C_L(\alpha, V)$$

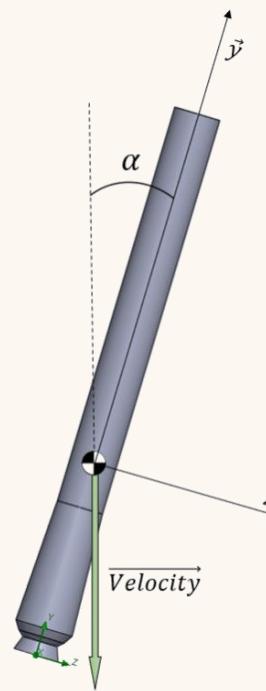


Fig. 19. Test model



Fig. 21. Drag Force and Lift Force as a function of angle of attack

- Aerodynamic tests

$$C_D(\alpha, V) \quad C_L(\alpha, V)$$

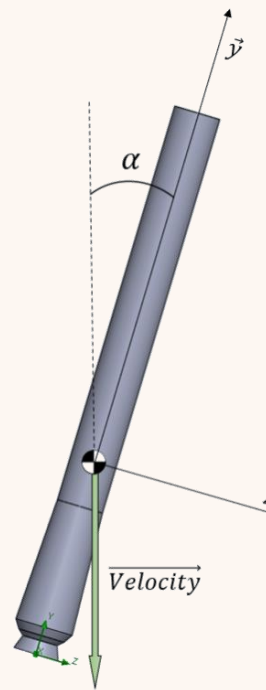


Fig. 19. Test model

Tab. 1. Aerodynamic force ratio

Angle	Force y	Force z	Drag force	Ratio/drag_force_0	Lift force	Ratio/Drag_force
0	2,65E+07	0,00E+00	2,65E+07	1	0,00E+00	0
1	2,63E+07	6,68E+05	2,63E+07	0,993	2,09E+05	0,008
3	2,55E+07	1,59E+06	2,55E+07	0,964	2,54E+05	0,010
5	2,60E+07	3,49E+06	2,62E+07	0,989	1,22E+06	0,047
10	2,55E+07	1,15E+07	2,71E+07	1,024	6,91E+06	0,255
15	2,56E+07	2,66E+07	3,16E+07	1,192	1,91E+07	0,605
20	2,56E+07	4,65E+07	4,00E+07	1,510	3,49E+07	0,873
25	2,59E+07	6,95E+07	5,28E+07	1,996	5,20E+07	0,985
30	2,55E+07	9,54E+07	6,97E+07	2,634	6,99E+07	1,002
40	2,27E+07	1,54E+08	1,17E+08	4,403	1,04E+08	0,888
50	1,66E+07	2,13E+08	1,74E+08	6,579	1,24E+08	0,715
60	1,08E+07	2,68E+08	2,38E+08	8,973	1,25E+08	0,525
70	6,43E+06	3,11E+08	2,94E+08	11,113	1,00E+08	0,341
80	3,14E+06	3,09E+08	3,05E+08	11,532	5,07E+07	0,166



- Aerodynamic tests

$$C_D(\alpha, V)$$

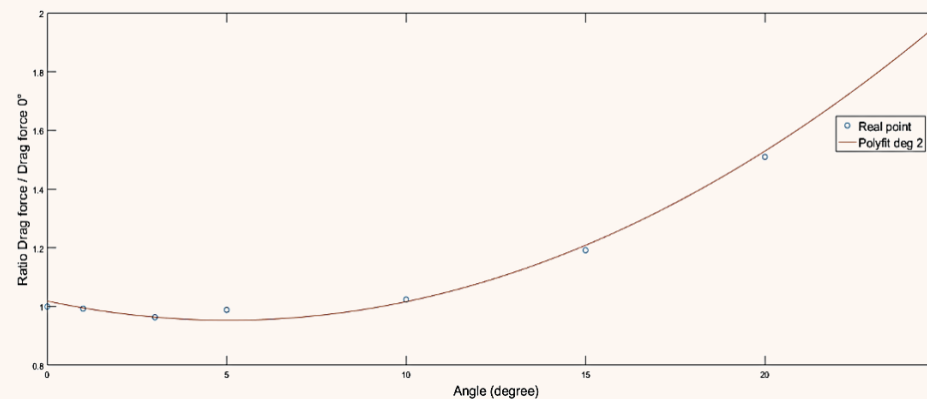


Fig. 22. Ratio of drag force to drag force for $\alpha = [0^\circ, 25^\circ]$

$$\text{Ratio}_1(\alpha) = 0.0026 * \alpha^2 - 0.0260 * \alpha + 1.0191 \quad (12)$$

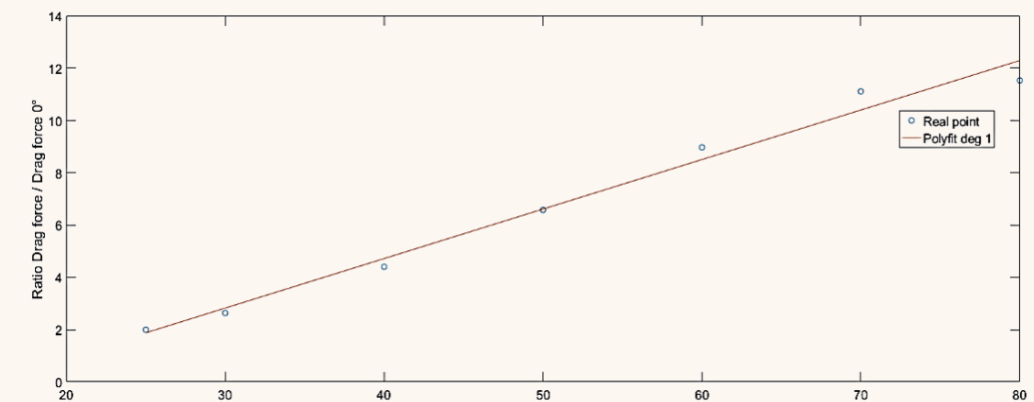


Fig. 23. Ratio of drag force to drag force for $\alpha = [25^\circ, 80^\circ]$

$$\text{Ratio}_2(\alpha) = 0.1894 * \alpha - 2.8591 \quad (13)$$

- Aerodynamic tests

$$C_L(\alpha, V)$$

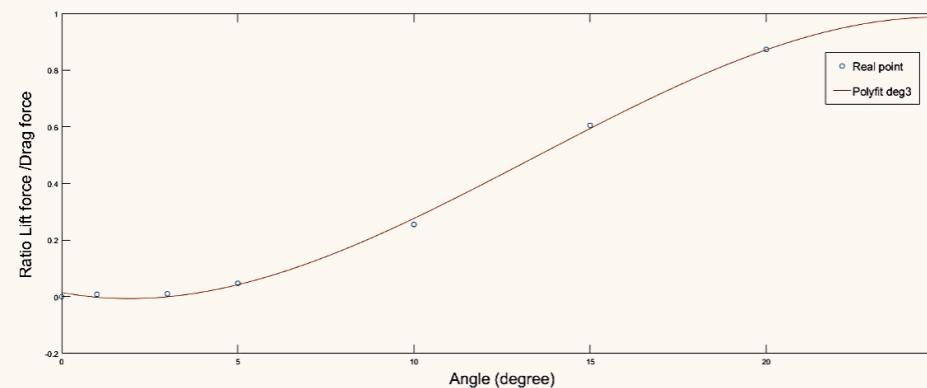


Fig. 24. Ratio of lift force to drag force for $\alpha=[0^\circ, 25^\circ]$

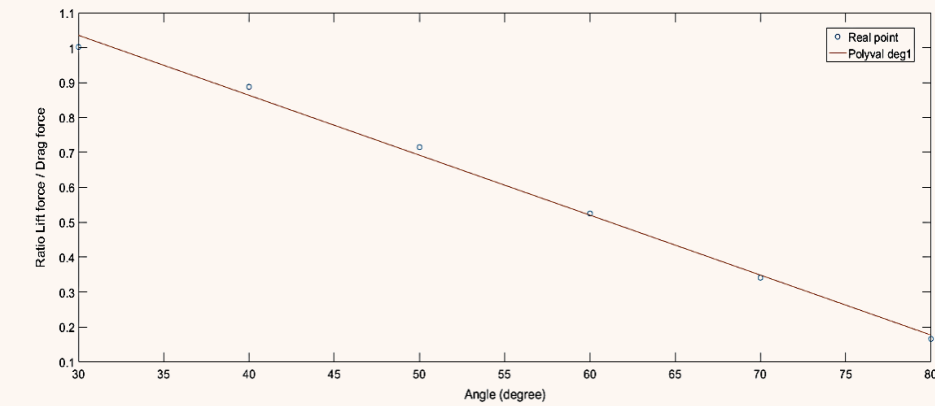


Fig. 25 Ratio of lift force to drag force for $\alpha=[25^\circ, 80^\circ]$

$$\text{Ratio}_4(\alpha) = -0.0002 * \alpha^3 + 0.0066 * \alpha^2 - 0.0234 * \alpha + 0.0148 \quad (14)$$

$$\text{Ratio}_5(\alpha) = -0.0172 * \alpha + 1.5508 \quad (15)$$



- Aerodynamic tests

$$C_D(\alpha, V)$$

$$C_L(\alpha, V)$$

$$q(y)$$

- MATLAB model

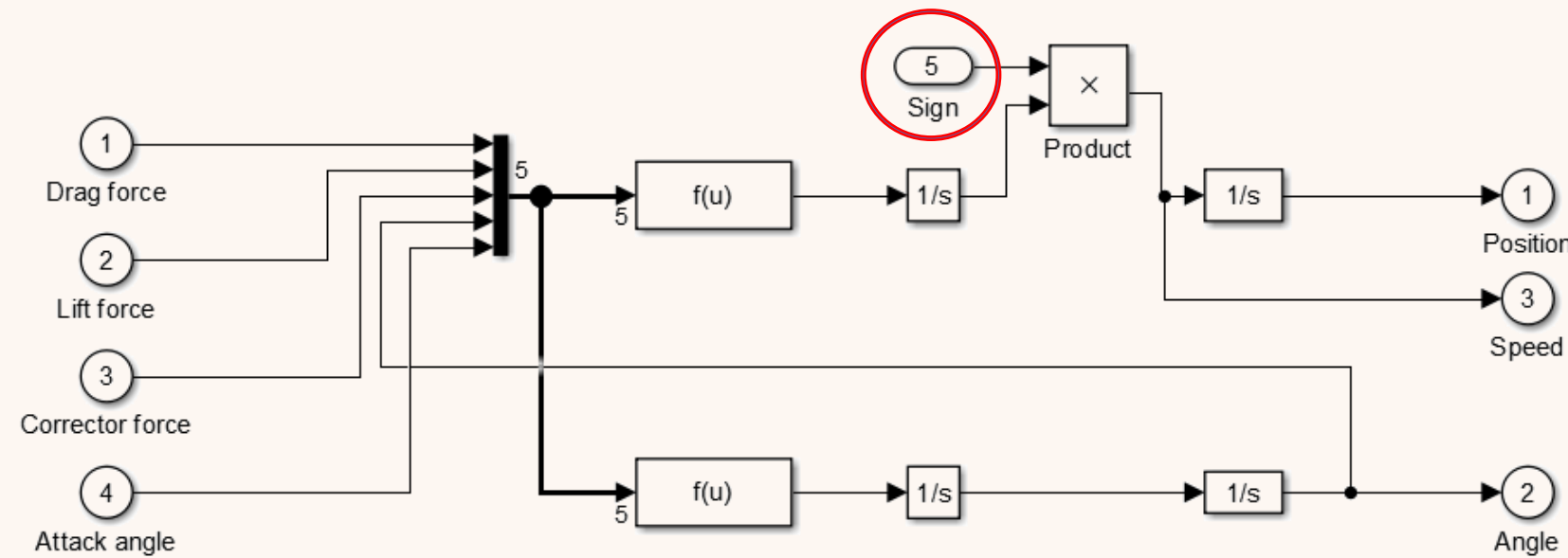


Fig. 26. MATLAB/Simulink model atmospheric re-entry

- MATLAB model

$$\alpha_{roll} = |\theta - \arctan\left(\frac{V_x}{V_y}\right)| \quad (16)$$

$$\alpha_{pitch} = |\theta - \arctan\left(\frac{V_z}{V_y}\right)| \quad (17)$$

Remark: Mathematic point N°2

$$\alpha = \arctan(\sqrt{\tan^2(pitch) + \tan^2(roll)}) \quad (23)$$

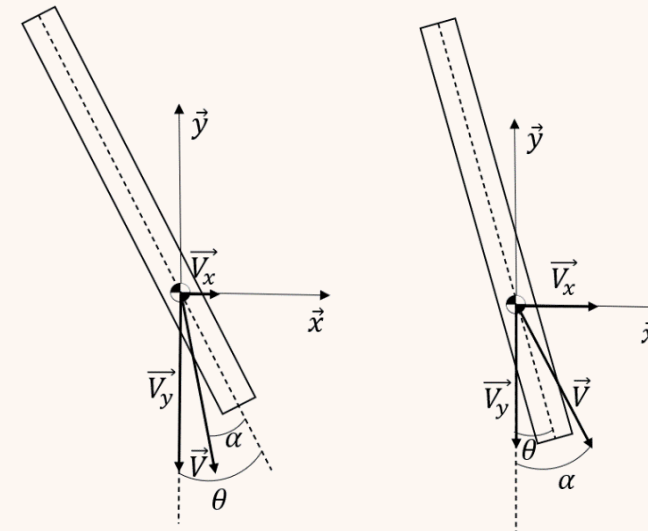


Fig. 27. Representation of the angle of attack

- Simulations and results

Parameter of the launcher during its re-entry phase :

Mass: 400 kg
Height: 7 m
Radius: 0.29 m
Inertia: $1650 \text{ kg} \cdot \text{m}^2$

The density of the Falcon 9 launcher is preserved.

Experimental conditions :

The initial altitude is 40 km
The initial speed is zero
Archimedes' strength is not considered
The wind is supposed to be zero

• Simulations and results

List of experiments:

- Free fall without atmosphere
- Free fall with atmosphere
- 2D control of the angle of attack
- 2D angle-of-attack control with sinusoidal control
- 2D control of the angle of attack with gate control
- 3D control of the angle of attack with a helical effect

Results of the experiments:

- Time of arrival
- Distance from the landing point to the vertical line

- Simulations and results

Free fall without atmosphere

$$t = \sqrt{\frac{2*h}{g}} = \sqrt{\frac{2*40000}{9.81}} = 90.3 \text{ s} \quad (24)$$

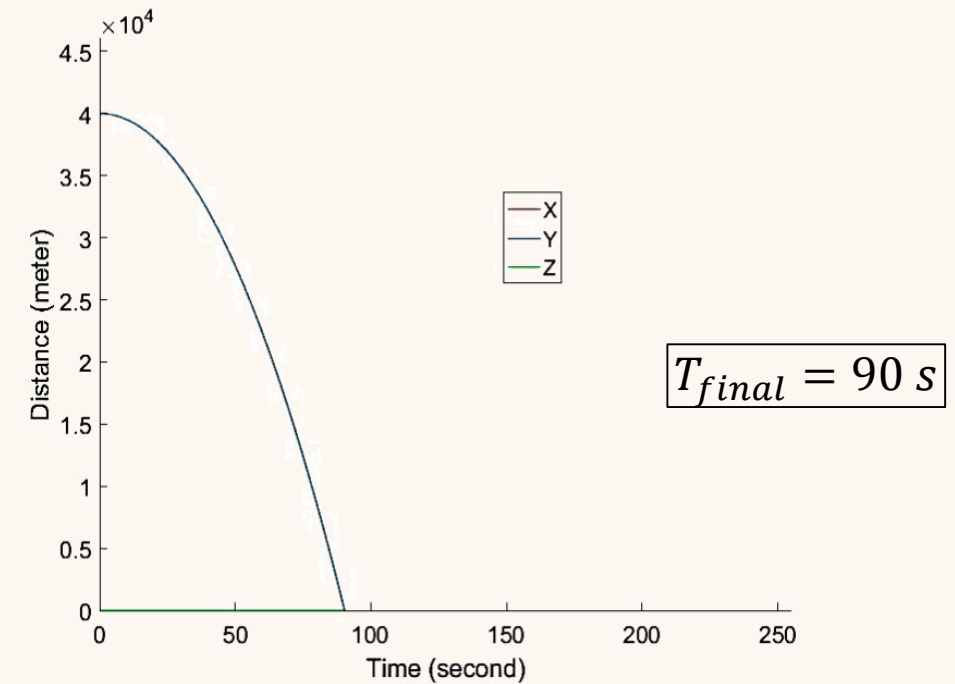


Fig. 29. Altitude as a function of time, free fall without atmosphere

- Simulations and results

Free fall with atmosphere

$$Ratio_{time} = \frac{Time_{touchdown}(\text{attack angle})}{Time_{touchdown_0}} \quad (25)$$

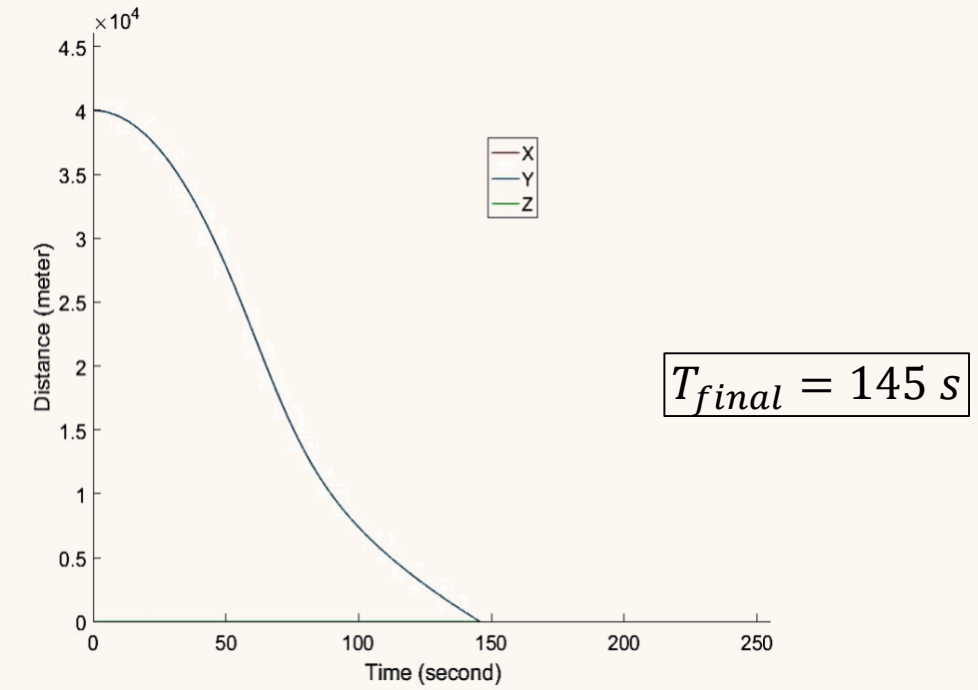


Fig. 30. Altitude as a function of time, fall with atmosphere

- Simulations and results

2D control of the angle of attack

$$Ratio_{time} = \frac{Time_{touchdown}(\text{attack angle})}{Time_{touchdown_0}} \quad (25)$$

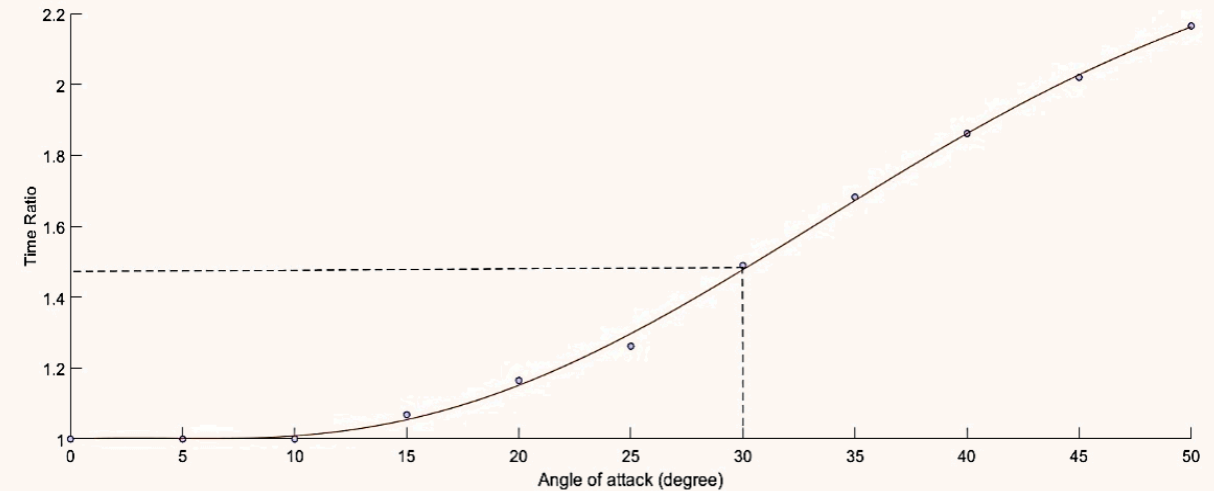


Fig. 31. Ratio curve as a function of angle of attack

- Simulations and results

2D control of the angle of attack

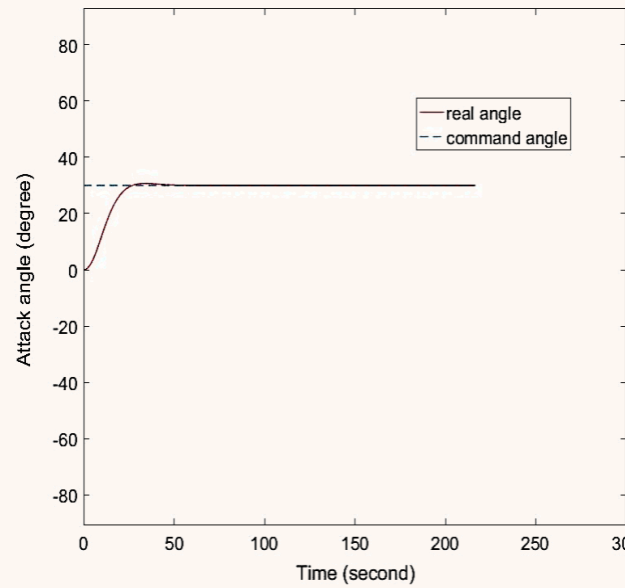


Fig. 32. Angle of attack, simple 2D control

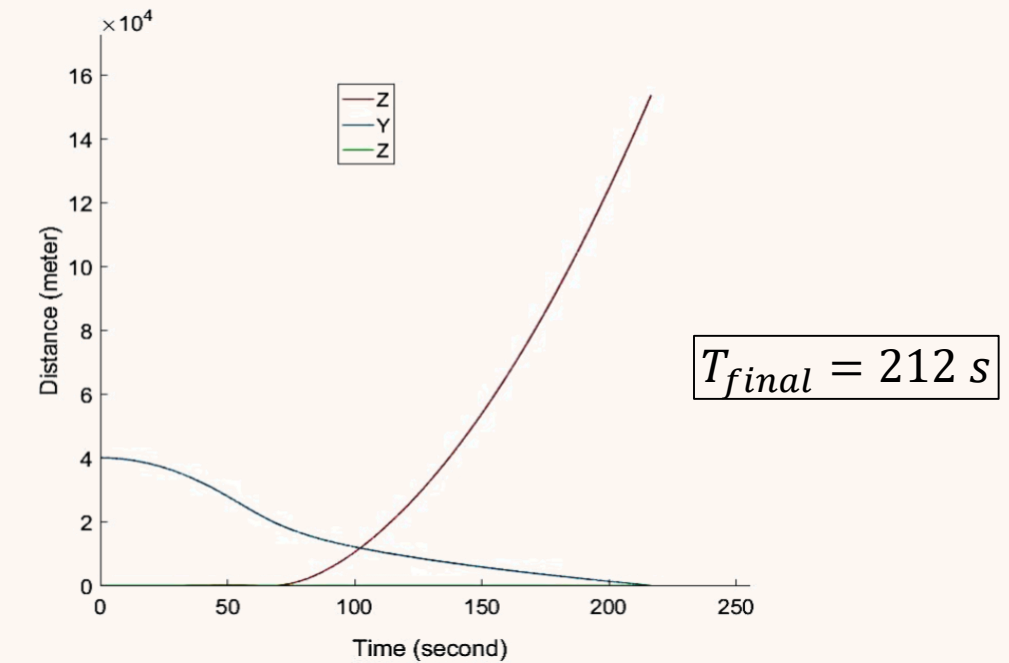


Fig. 33. Altitude as a function of time, simple 2D control

- Simulations and results

2D angle-of-attack control with sinusoidal control

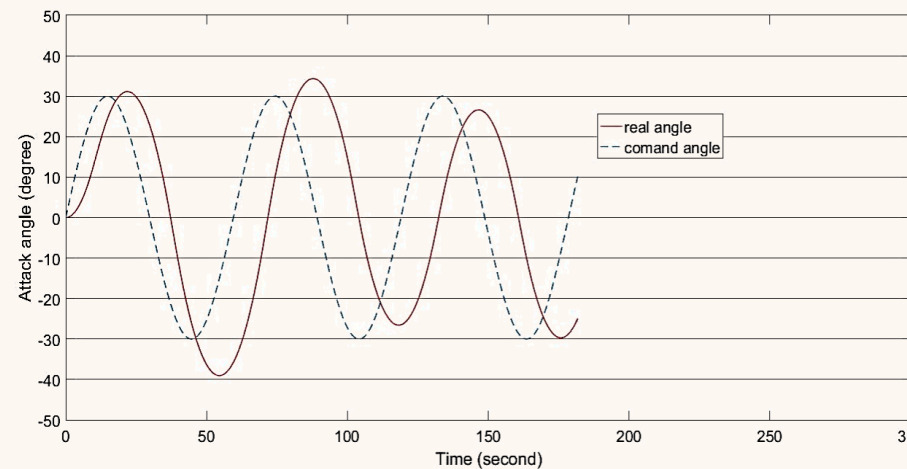


Fig. 34. Attack angle, 2D sinusoidal control

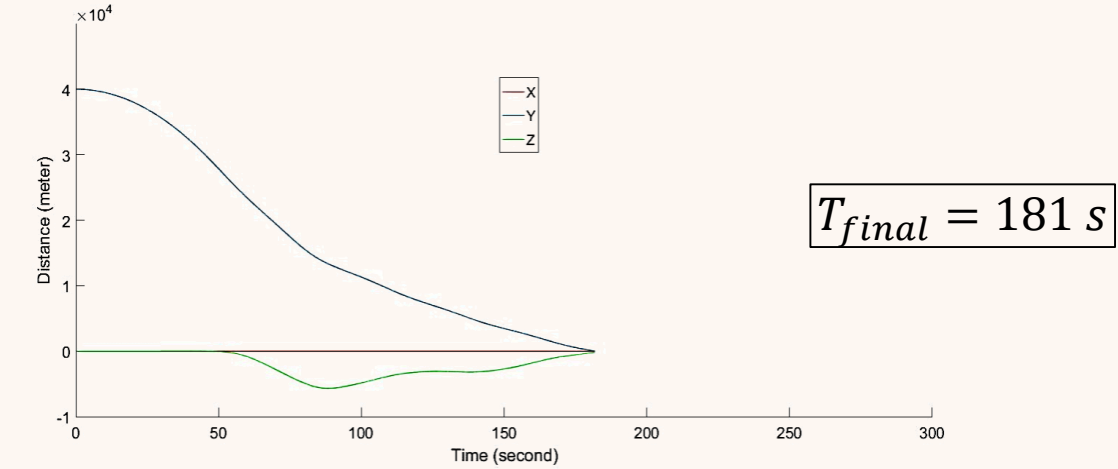


Fig. 35. Altitude as a function of time, 2D sinusoidal control

- Simulations and results

2D control of the angle of attack with a gate control

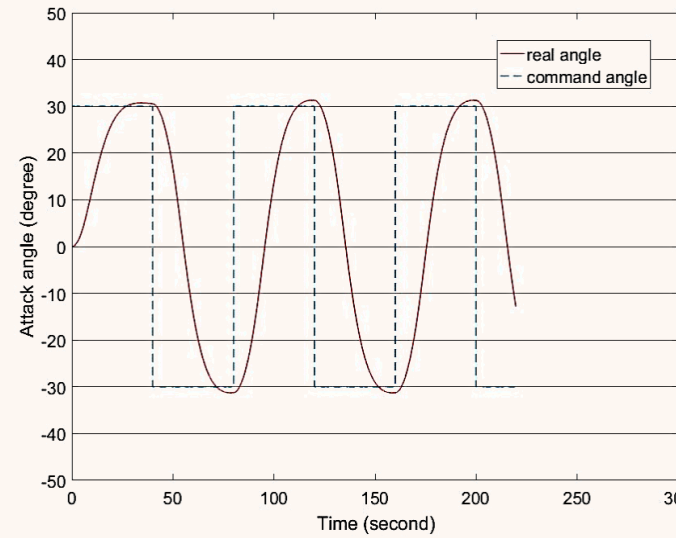
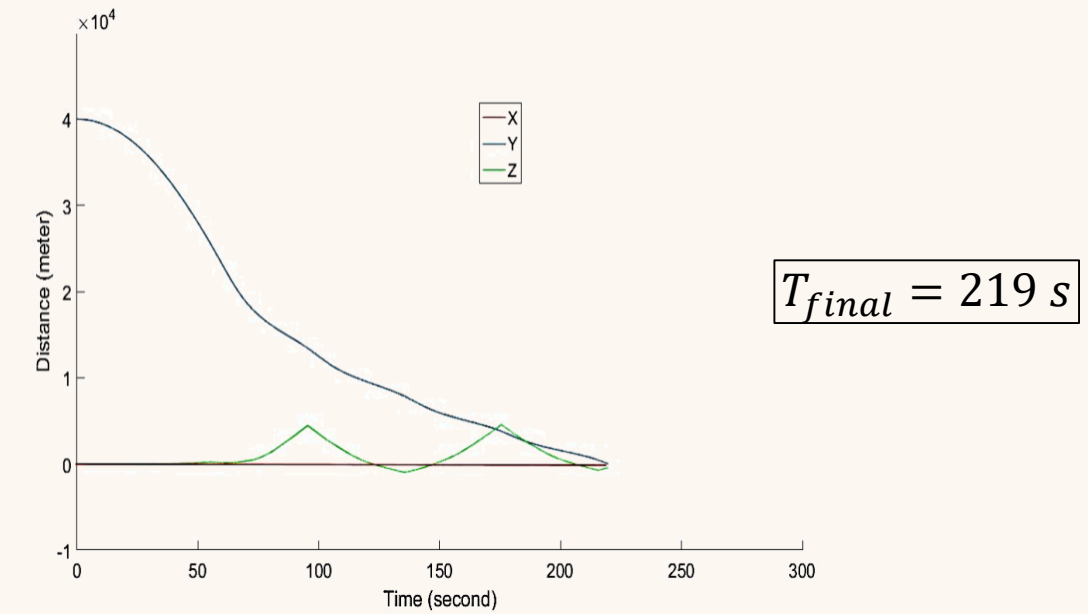


Fig. 36. Attack angle, short gate 2D control



$$T_{final} = 219 \text{ s}$$

Fig. 37. Altitude as a function of time, 2D short gate control

- Simulations and results

2D control of the angle of attack with a gate control

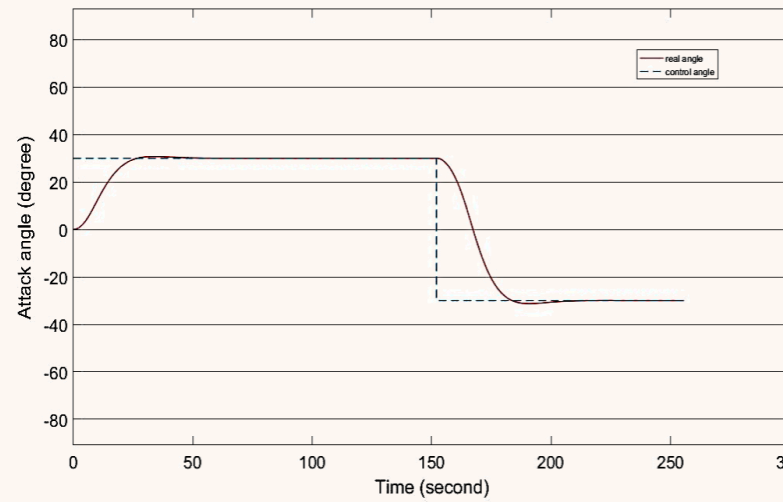


Fig. 38. Attack angle, large gate 2D control

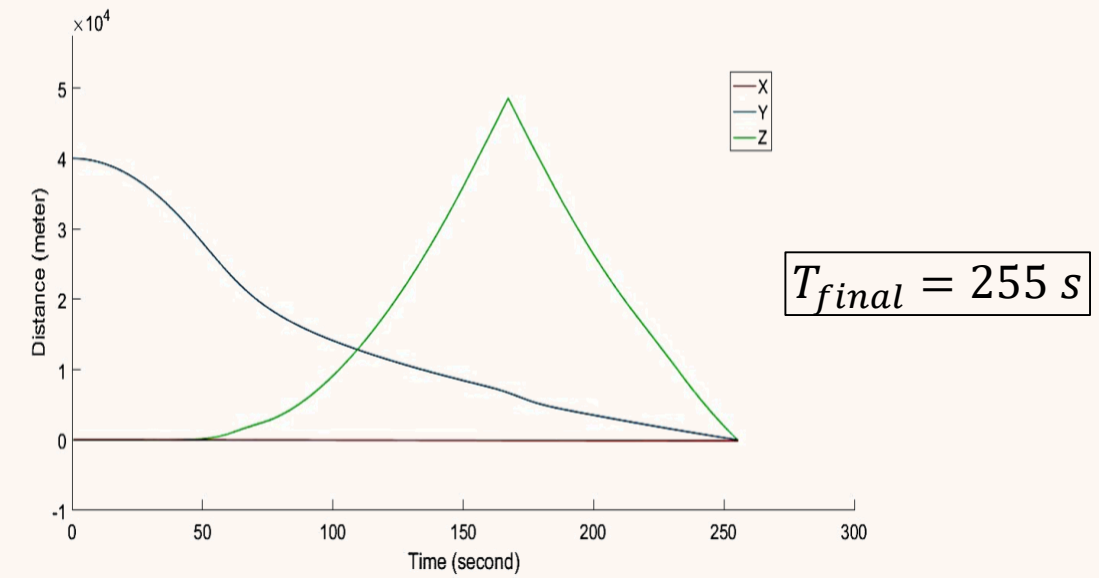


Fig. 39. Altitude as a function of time, 2D large gate control

- Simulations and results

3D control of the angle of attack with a helical effect

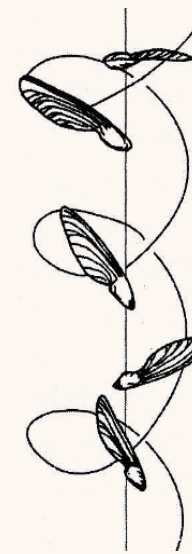


Fig. 40. Trajectory of a maple fruit

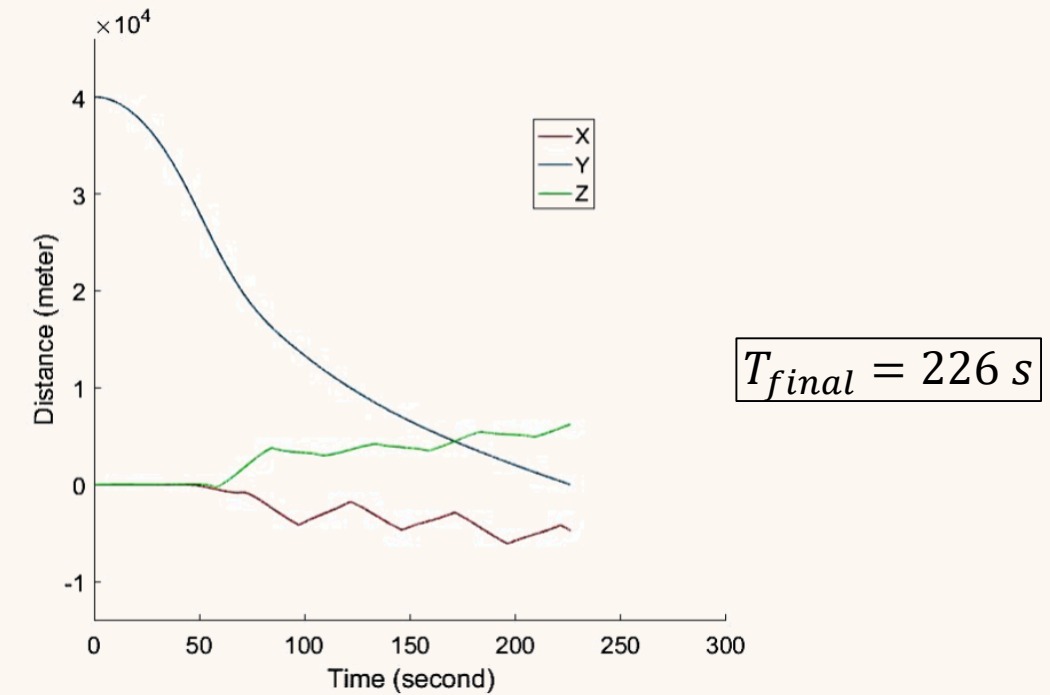


Fig. 41. Altitude as a function of time, 3D helical control

- Simulations and results

3D control of the angle of attack with a helical effect

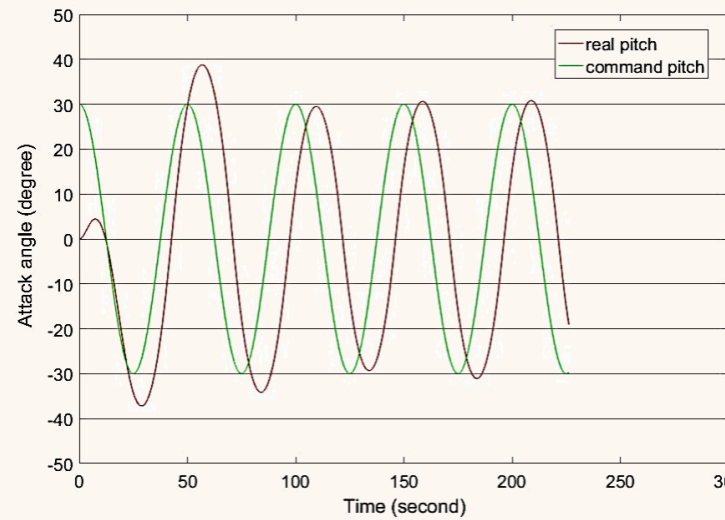


Fig. 42. Angle of attack (pitch)

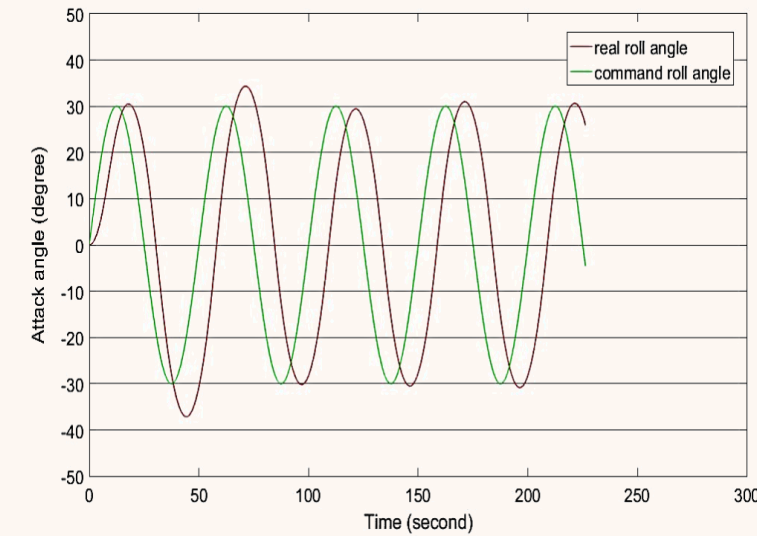


Fig. 43. Angle of attack (roll)

- Simulations and results

3D control of the angle of attack with a helical effect

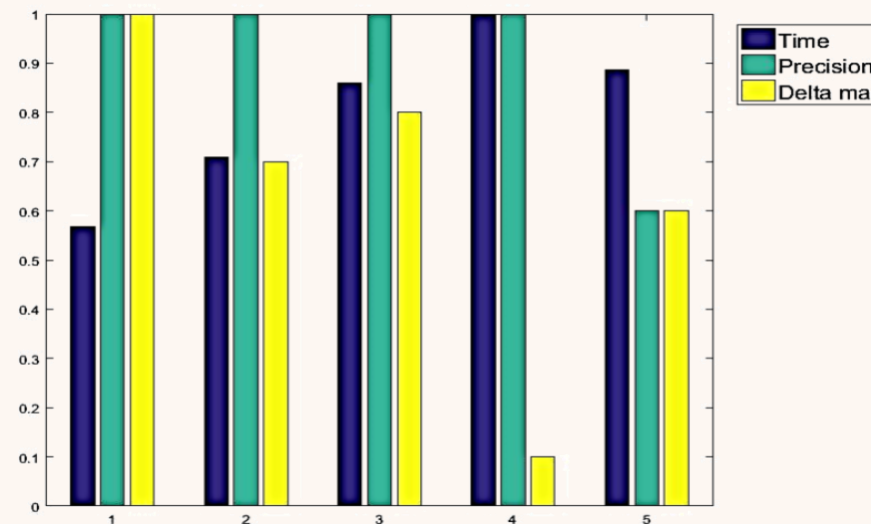


Fig. 44. Comparison chart

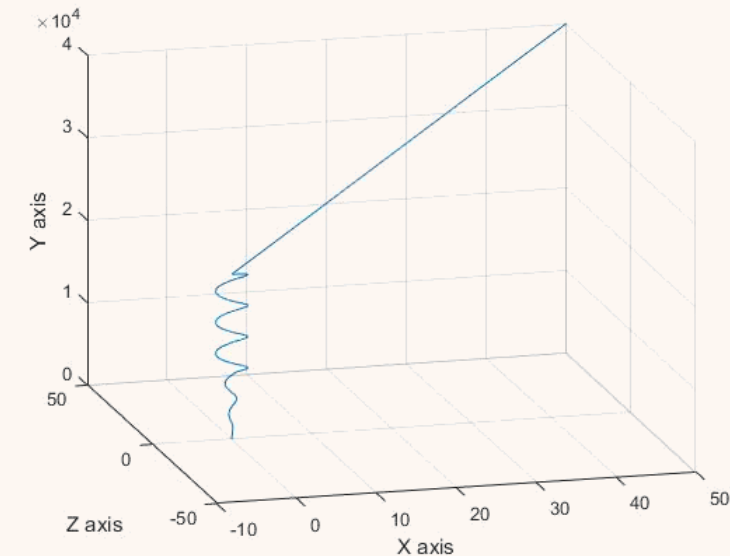


Fig. 45. Atmospheric re-entry idea



Summary

- Improvement RLV shape design
- Trajectory design and simulation
- End phase control design
- Validation of end phase control



Summary

- Improvement RLV shape design
- Trajectory design and simulation
- End phase control design
 - Presentation and equation of model
 - MATLAB model
 - Balance control
 - Altitude control
 - Control parameter
 - Simulation and results
- Validation of end phase control

- Presentation and equation of model

Length: L

Mass: m

Gravity: $g = 9.81 \text{ m/s}^2$

The angle between the vertical axis and the axis of the launcher: φ

$$\text{The inertia of the cylinder on the radial axes } I = \frac{m}{4} \left(R^2 + \frac{h^2}{3} \right)$$

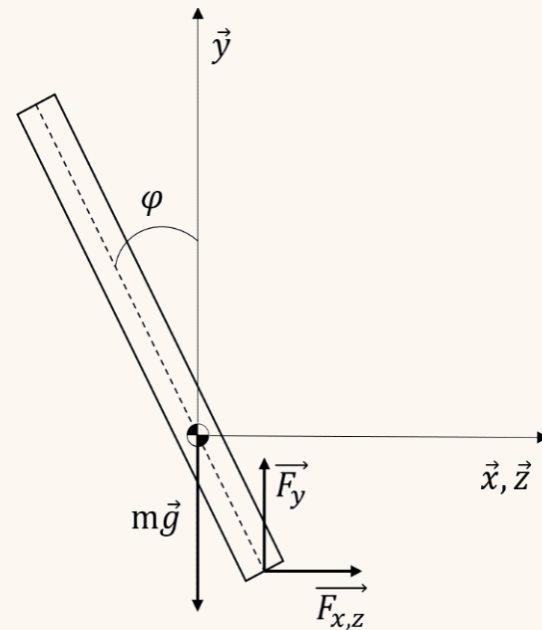


Fig. 46. Physical model of the RLV
during the landing phase

- Presentation and equation of model

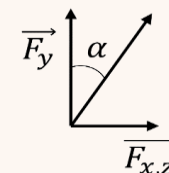
$$m \cdot \ddot{x}_G = Fx \quad (26)$$

$$m \cdot \ddot{y}_G = Fy - m \cdot g \quad (27)$$

$$I \cdot \ddot{\varphi} = (\frac{L}{2}) \cdot \cos(\varphi) \cdot Fx + (\frac{L}{2}) \cdot \sin(\varphi) \cdot Fy \quad (28)$$

$$\ddot{x}_G = \ddot{x} - (\frac{L}{2}) \cdot \ddot{\varphi} \cdot \cos(\varphi) + (\frac{L}{2}) \cdot \dot{\varphi}^2 \cdot \sin(\varphi) \quad (29)$$

$$\ddot{y}_G = \ddot{y} - (\frac{L}{2}) \cdot \ddot{\varphi} \cdot \sin(\varphi) - (\frac{L}{2}) \cdot \dot{\varphi}^2 \cdot \cos(\varphi) \quad (30)$$



$$Fx = F \cdot \sin(\alpha) \quad (31)$$

$$Fy = F \cdot \cos(\alpha) \quad (32)$$

$$Fx = m \cdot \ddot{x} - m \cdot \frac{L}{2} \cdot \ddot{\varphi} \cdot \cos(\varphi) + m \cdot (\frac{L}{2}) \cdot \dot{\varphi}^2 \cdot \sin(\varphi) \quad (33)$$

$$m \cdot \ddot{x} = Fx + m \cdot \frac{L}{2} \cdot (\ddot{\varphi} \cdot \cos(\varphi) - \dot{\varphi}^2 \cdot \sin(\varphi)) \quad (34)$$

$$Fy = m \cdot g + m \cdot \ddot{y} - m \cdot \frac{L}{2} \cdot \ddot{\varphi} \cdot \cos(\varphi) + m \cdot (\frac{L}{2}) \cdot \dot{\varphi}^2 \cdot \sin(\varphi) \quad (35)$$

$$m \cdot \ddot{y} = -Fy - m \cdot g + m \cdot \frac{L}{2} \cdot \ddot{\varphi} \cdot \cos(\varphi) - m \cdot (\frac{L}{2}) \cdot \dot{\varphi}^2 \cdot \sin(\varphi) \quad (36)$$

$$\begin{aligned} I \cdot \ddot{\varphi} = & (\frac{L}{2}) \cdot \cos(\varphi) \cdot (m \cdot \ddot{x} - m \cdot \frac{L}{2} \cdot \ddot{\varphi} \cdot \cos(\varphi) + m \cdot (\frac{L}{2}) \cdot \dot{\varphi}^2 \cdot \sin(\varphi)) \\ & + (\frac{L}{2}) \cdot \sin(\varphi) \cdot (m \cdot g - m \cdot \frac{L}{2} \cdot \ddot{\varphi} \cdot \cos(\varphi) + m \cdot (\frac{L}{2}) \cdot \dot{\varphi}^2 \cdot \sin(\varphi)) \end{aligned} \quad (37)$$

$$\left(m \cdot (\frac{L}{2})^2 + I \right) \cdot \ddot{\varphi} = m \cdot (\frac{L}{2}) \cdot (\ddot{x} \cdot \cos(\varphi) + g \cdot \sin(\varphi)) \quad (38)$$

- MATLAB model

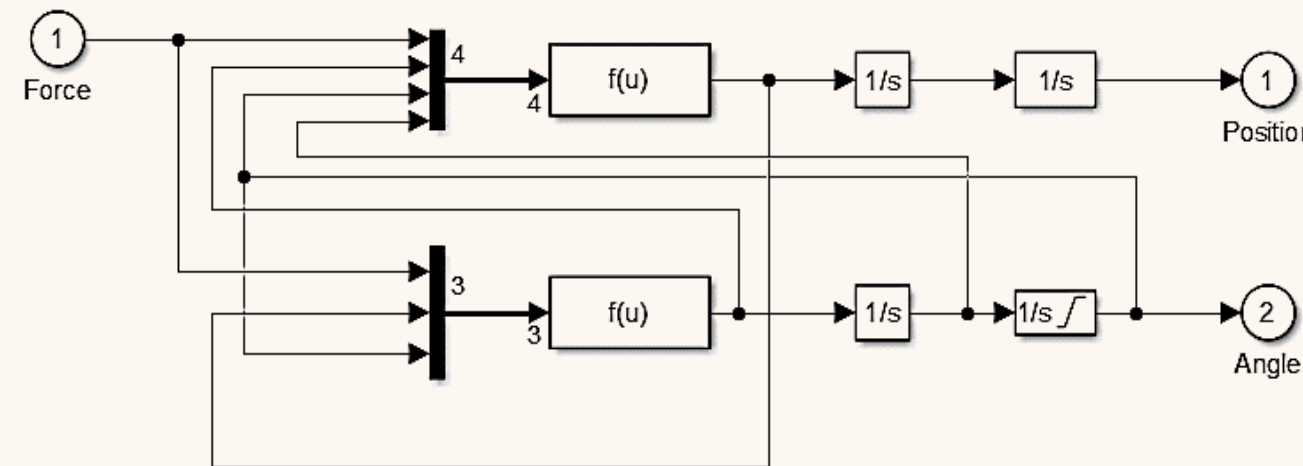


Fig. 47. MATLAB/Simulink model of RLV flight without aerodynamic effect

- MATLAB model

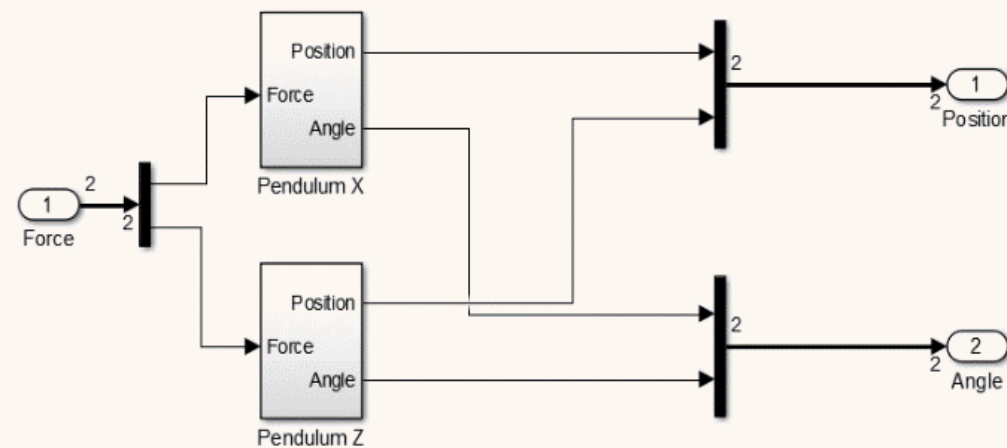


Fig. 48. Switching from 2D to 3D model

- Balance control

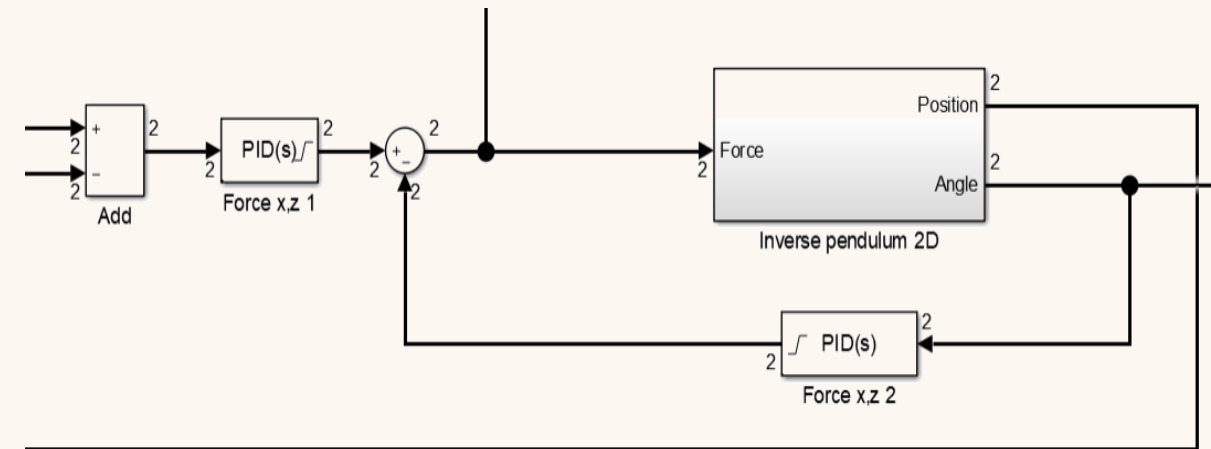


Fig. 49. PID control system for RLV balance

- Balance control

$$\rho_{falcon9} = 211.66 \text{ kg.m}^{-3} \quad (39)$$

$$\text{Mass} = \rho_{falcon9} * \pi * r^2 * \text{Length} \quad (40)$$

$$\text{Radius} = \text{Length}/23,8 \quad (41)$$

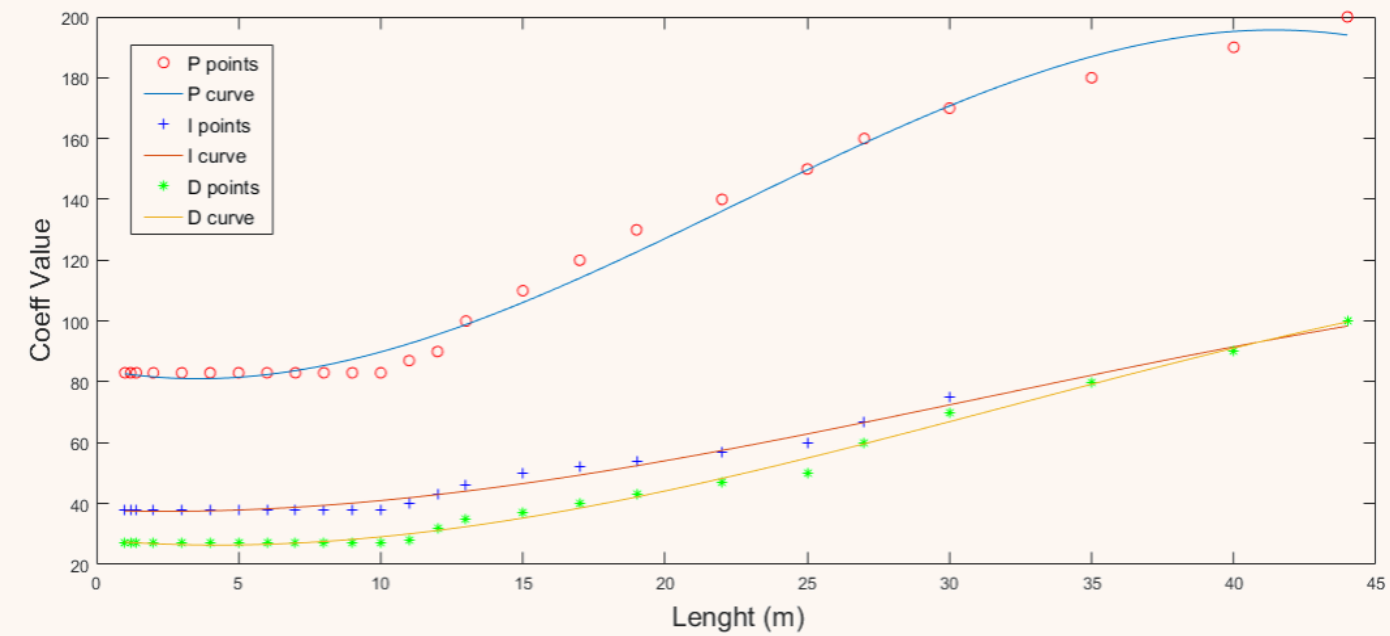


Fig. 50. PID coefficients as a function of RLV dimensions

- Balance control

$$P(L) = -0.0042 * L^3 + 0.2854 * L^2 - 1.8742 * L + 84.3006 \quad (42)$$

$$I(L) = -0.0008 * L^3 + 0.0727 * L^2 - 0.3354 * L + 37.8584 \quad (43)$$

$$D(L) = -0.0011 * L^3 + 0.1017 * L^2 - 0.8084 * L + 28.0509 \quad (44)$$

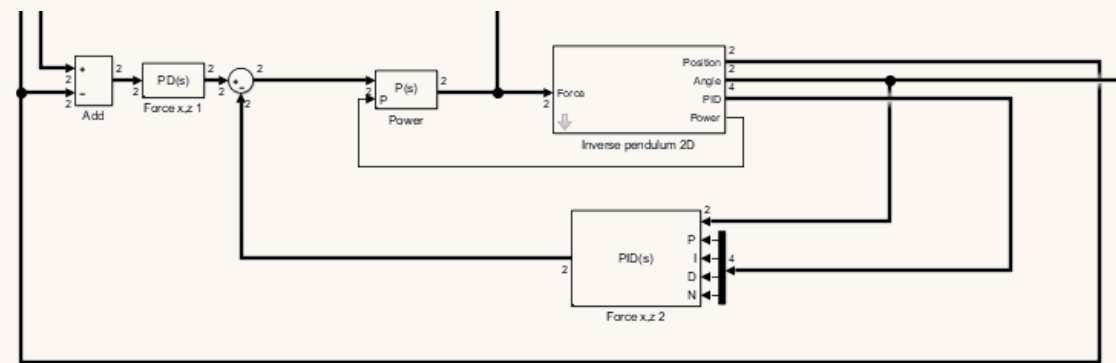


Fig. 51. PID control system for RLV balance with coefficient apatation

- Altitude control

$$m \cdot \ddot{y}_G = F_y - m \cdot g \quad (27)$$

$$F_y = F \cdot \cos(\alpha) \quad (32)$$

$$m \cdot \ddot{y}_G = F \cdot \cos(\alpha) - m \cdot g \quad (45)$$

$$\alpha = \arctan(\sqrt{\tan^2(\text{pitch}) + \tan^2(\text{roll})}) \quad (23)$$

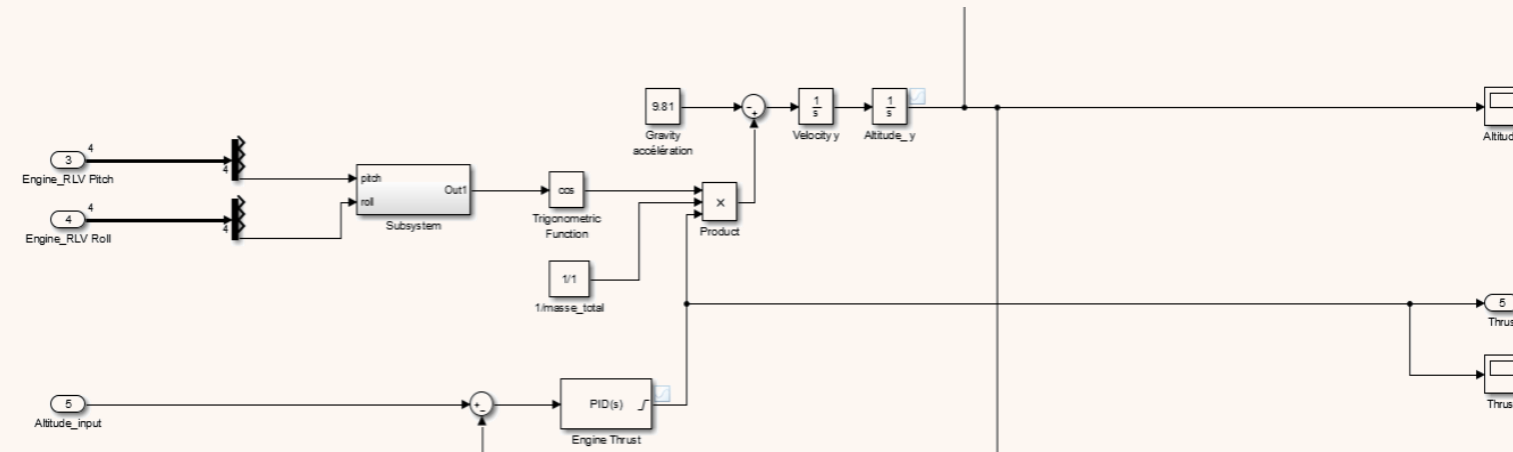


Fig. 52. PID control system for RLV altitude

- Altitude control

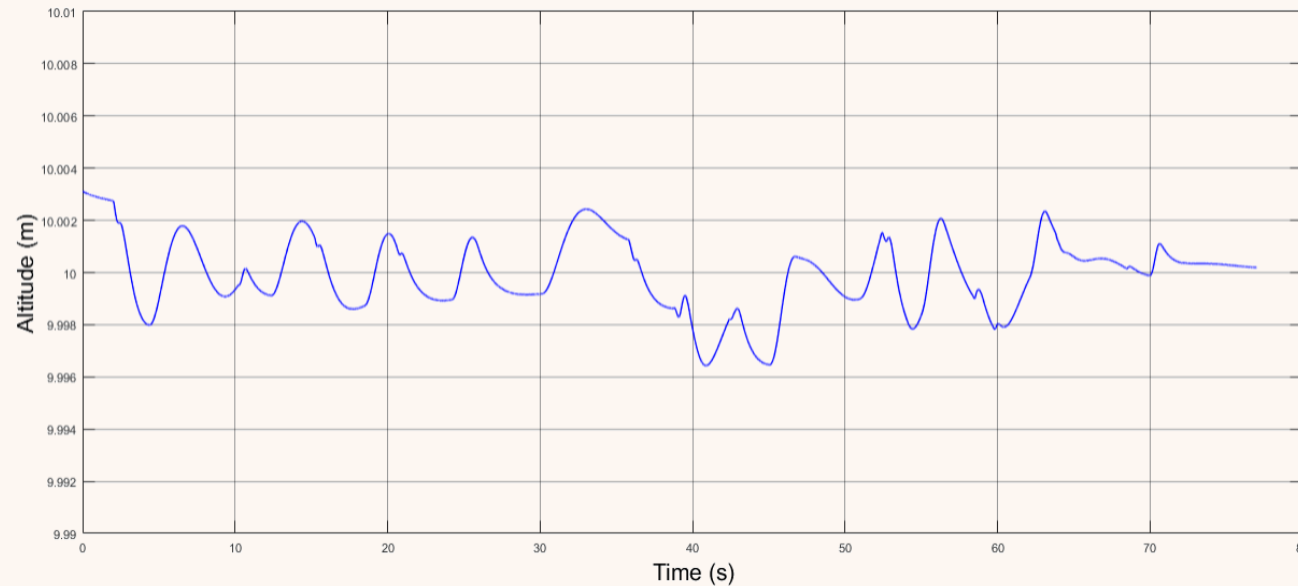


Fig. 53. Variation of the RLV's altitude during lots of lateral displacements

- Altitude control

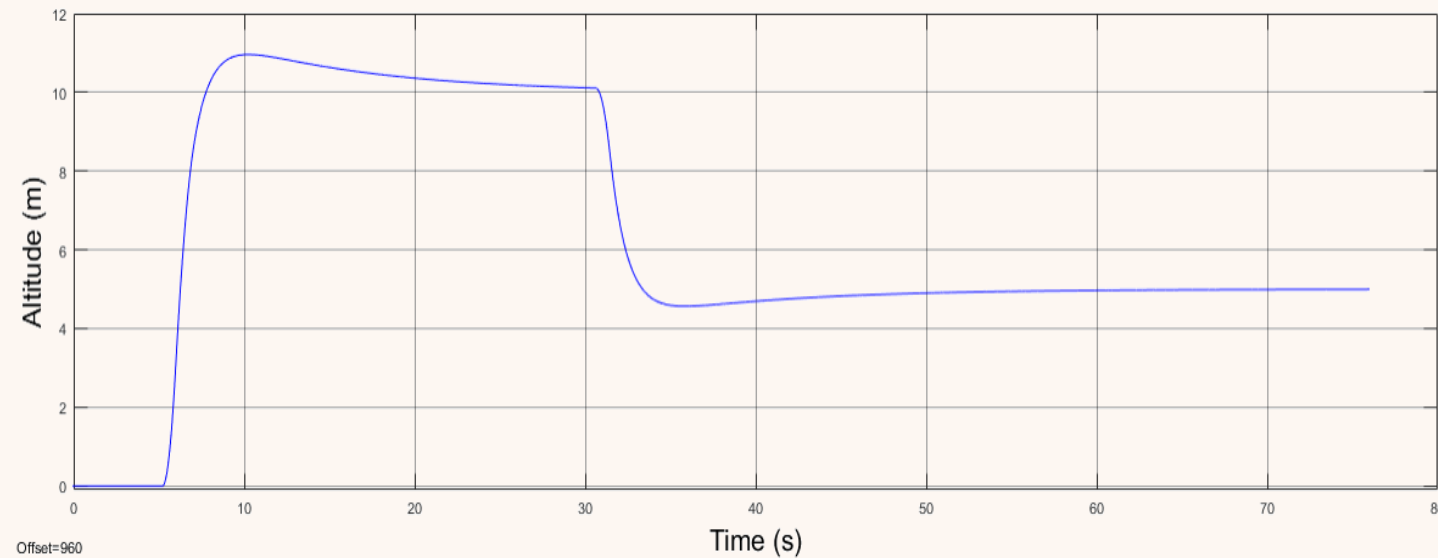


Fig. 54. Altitude variation at a gate [+ 10m] then [- 5m].

- Control parameter

$$Fx = F \cdot \sin(\alpha) \quad (31)$$

$$Fy = F \cdot \cos(\alpha) \quad (32)$$

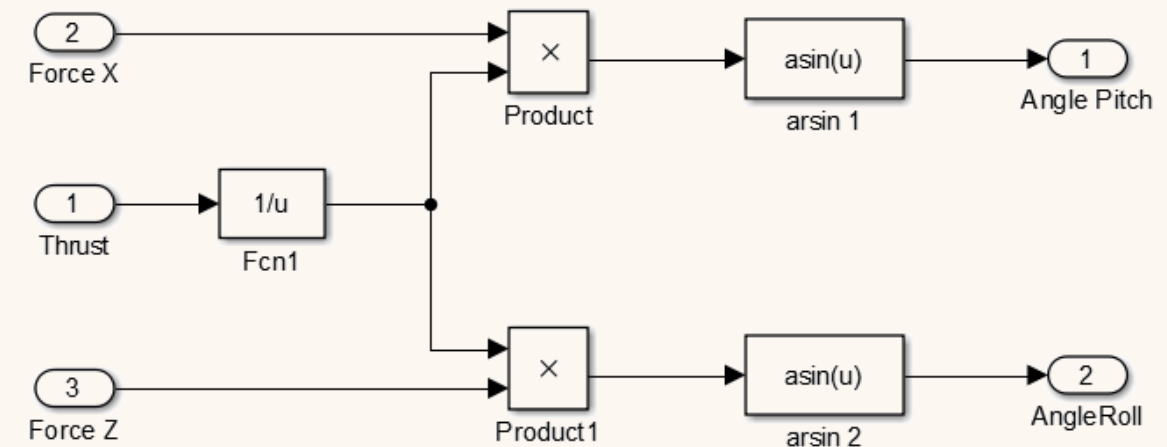


Fig. 55. Determination of engine thrust angles

- Simulations and results

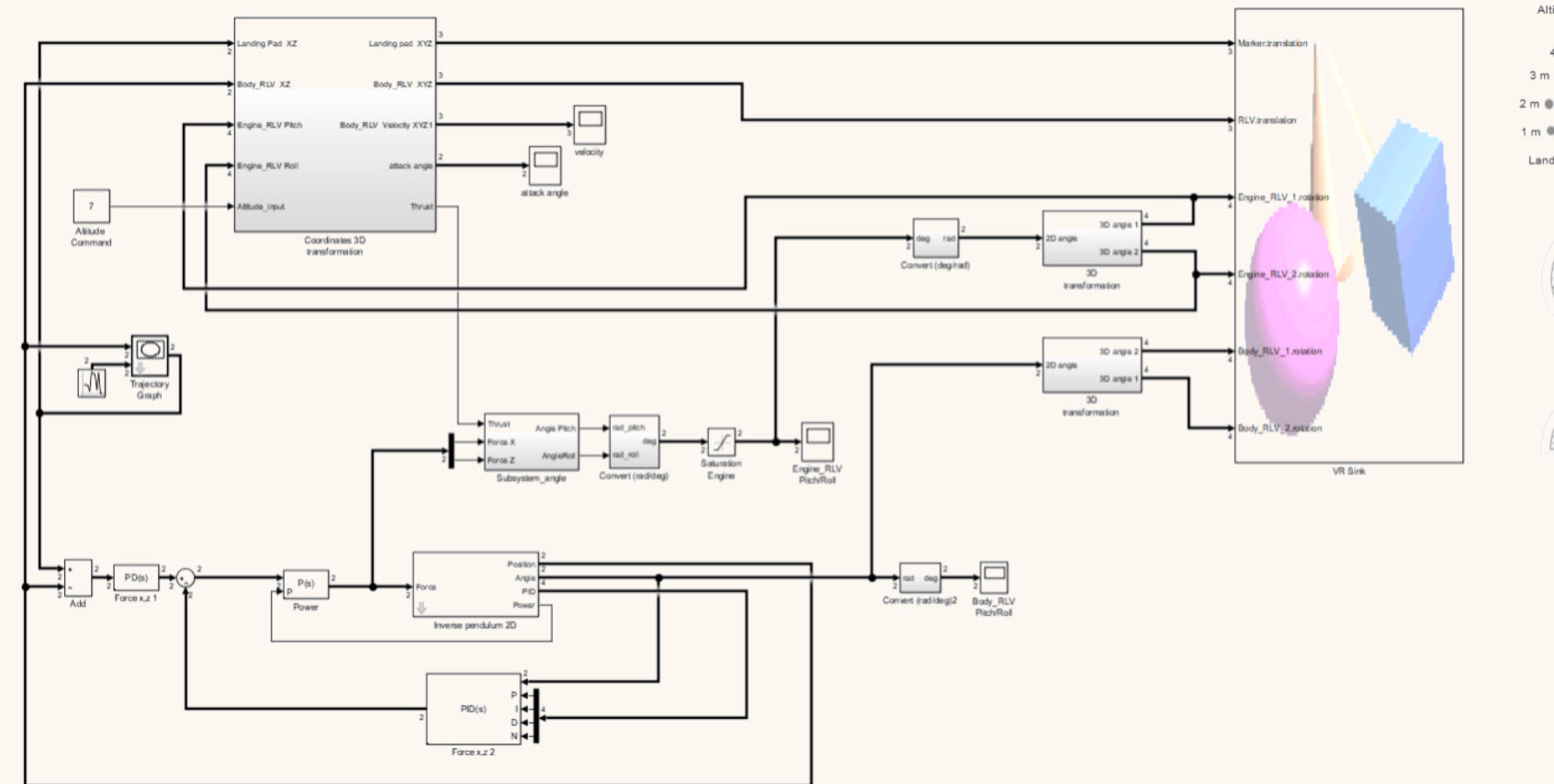


Fig. 56. Entire MATLAB/Simulink model for RLV stability control during landing phase

- Simulations and results

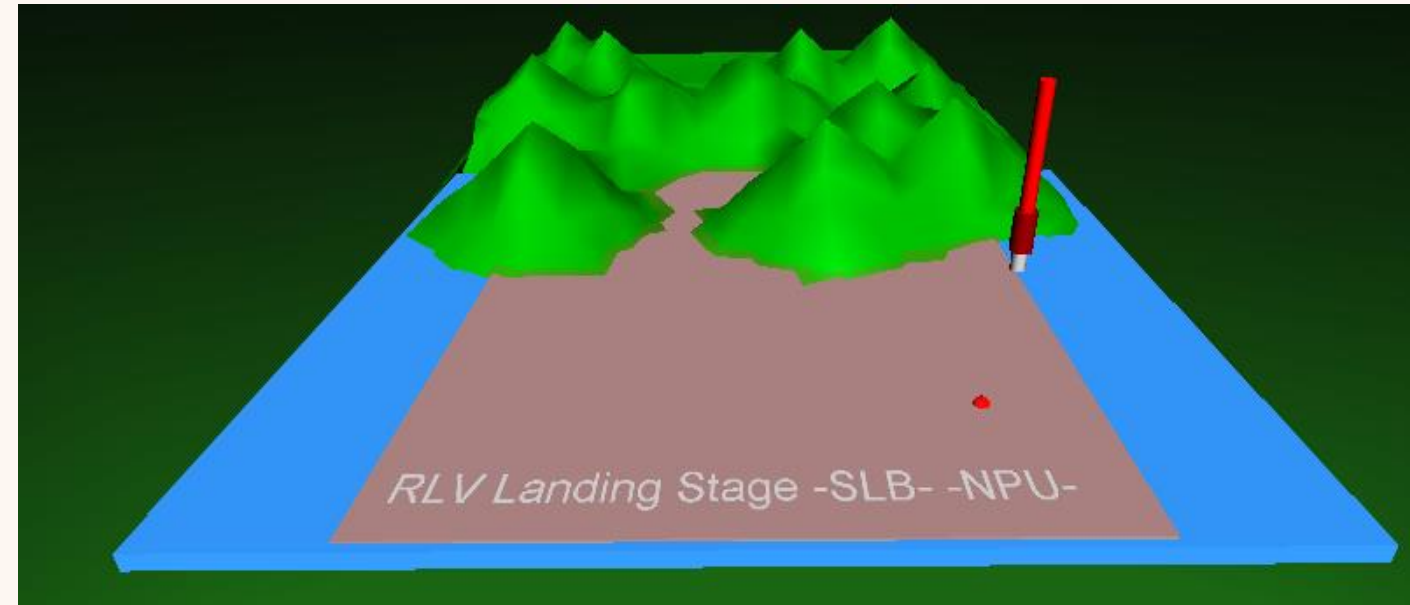


Fig. 57. 3D World to simulate our model

- Simulations and results

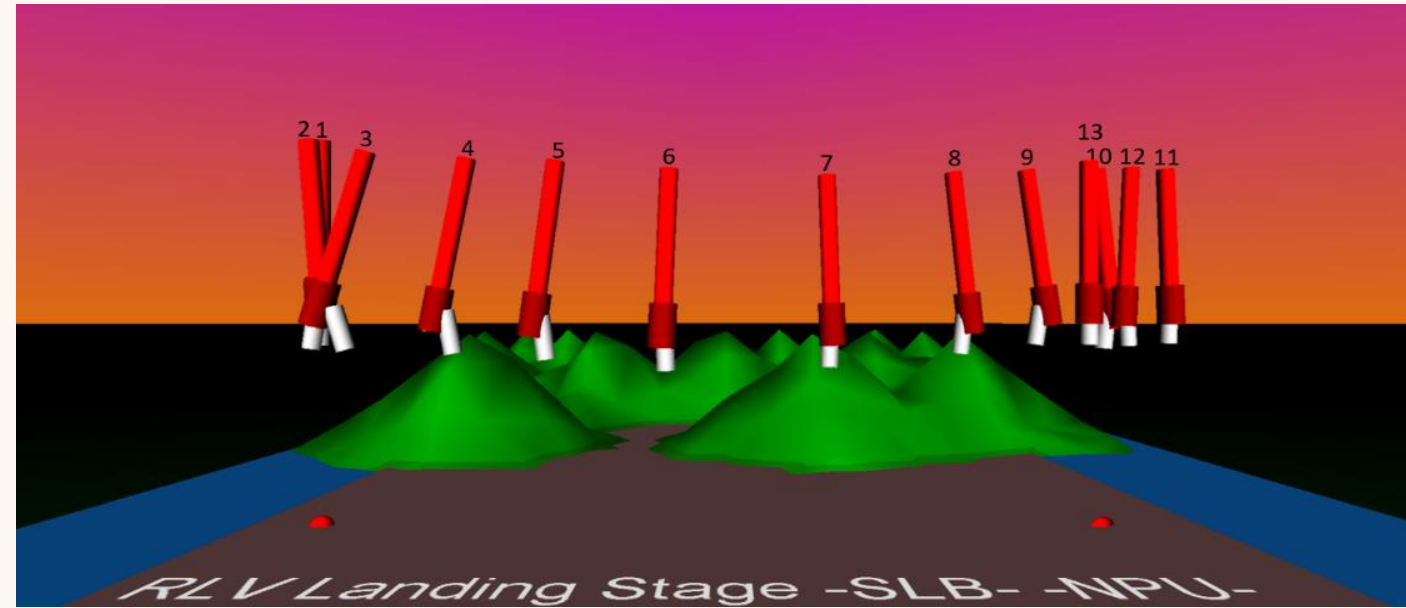
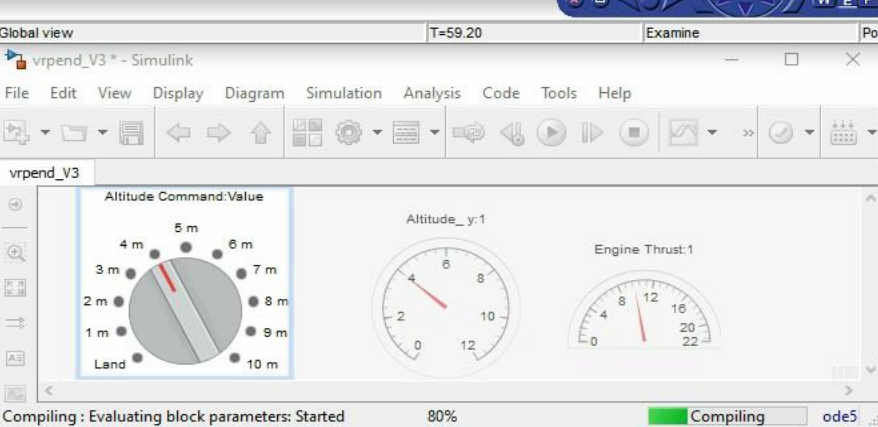
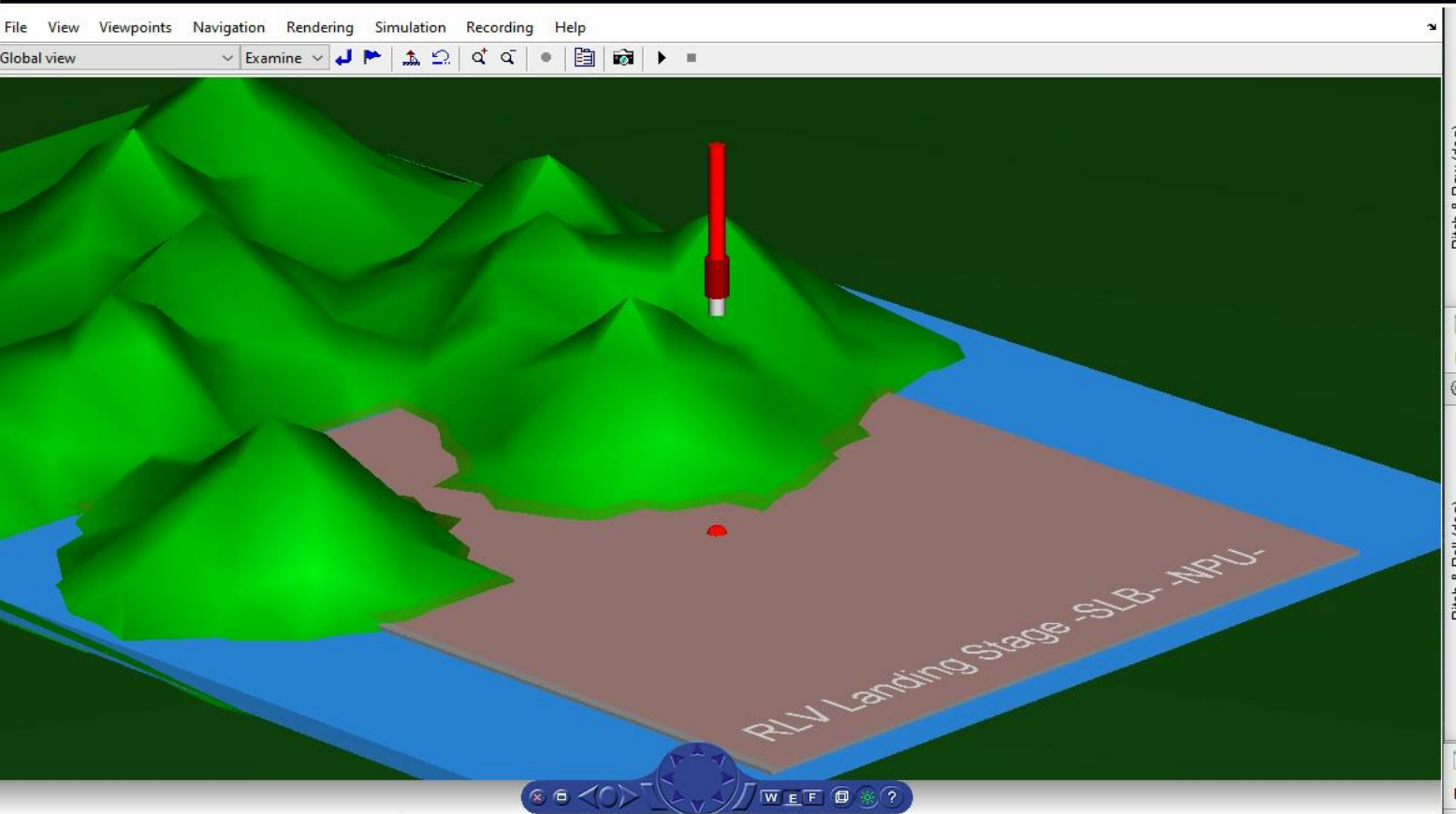


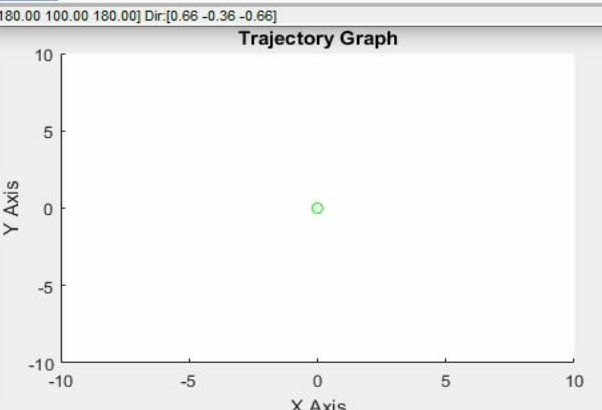
Fig. 58. Stroboscopic view of a movement



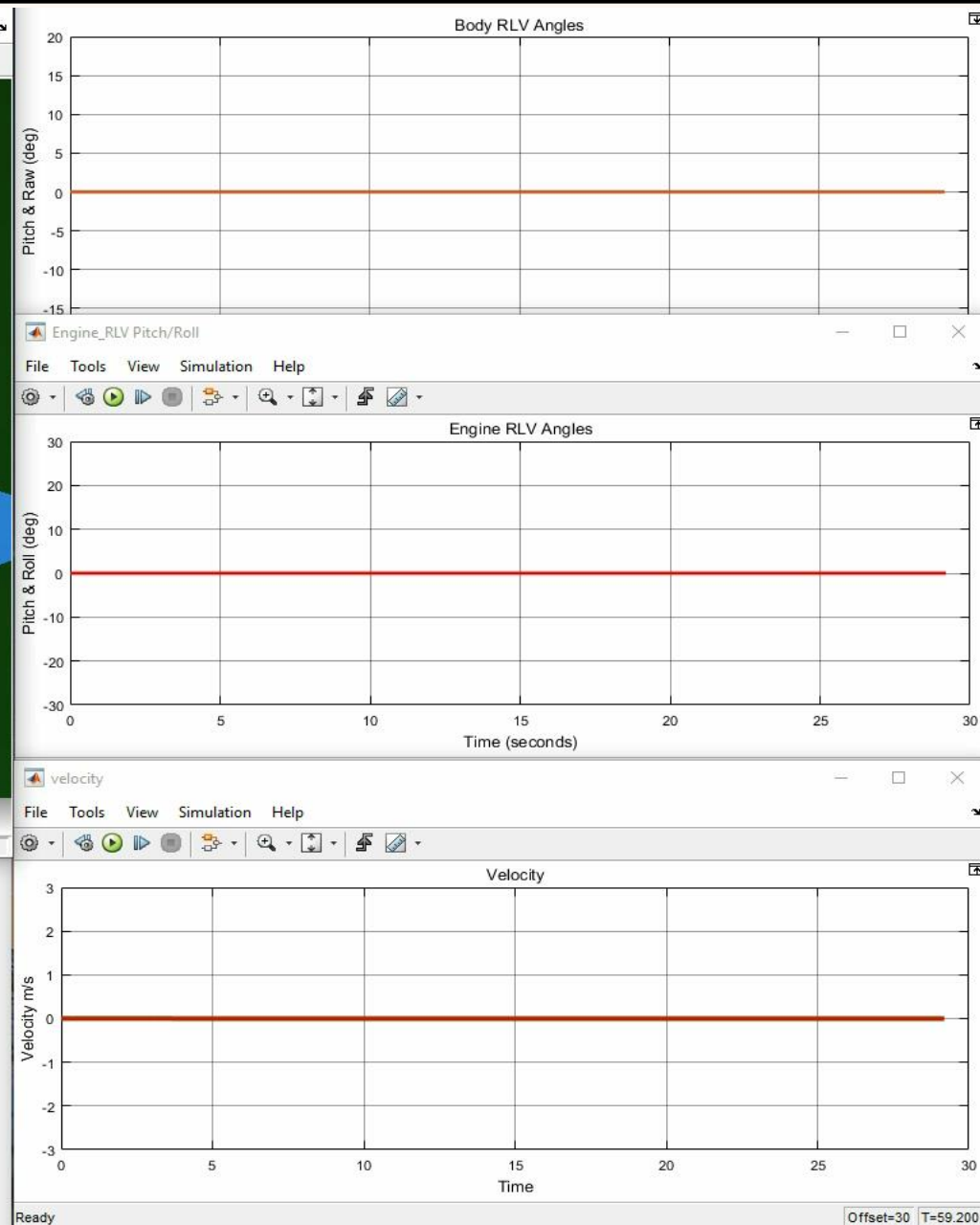
Improvement RLV shape design



Trajectory design and simulation



End phase control design



Validation of end phase control



Summary

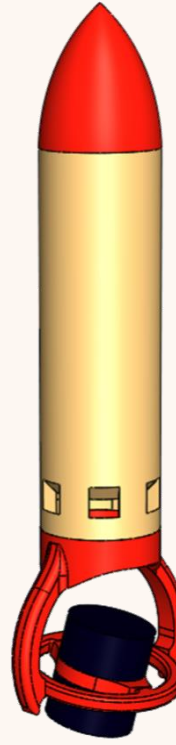
- Improvement RLV shape design
- Trajectory design and simulation
- End phase control design
- Validation of end phase control



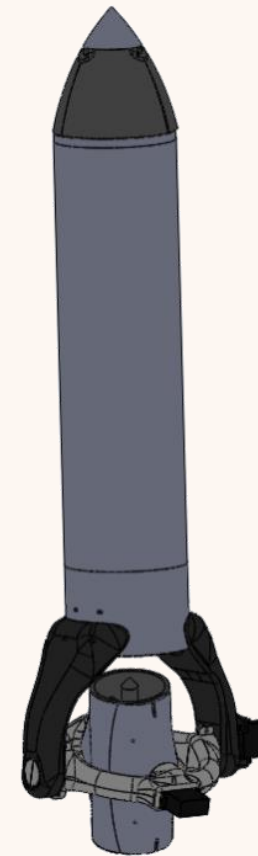
Summary

- Improvement RLV shape design
- Trajectory design and simulation
- End phase control design
- Validation of end phase control
 - Model 1
 - Model 2
 - Model 3
 - Model 4
 - Engine system
 - Other equipment

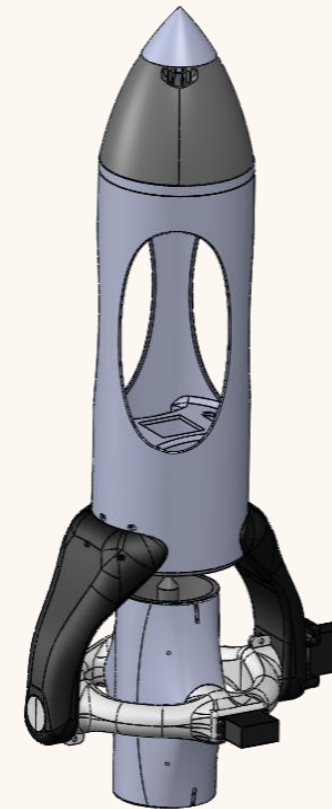
Model 1



Model 2



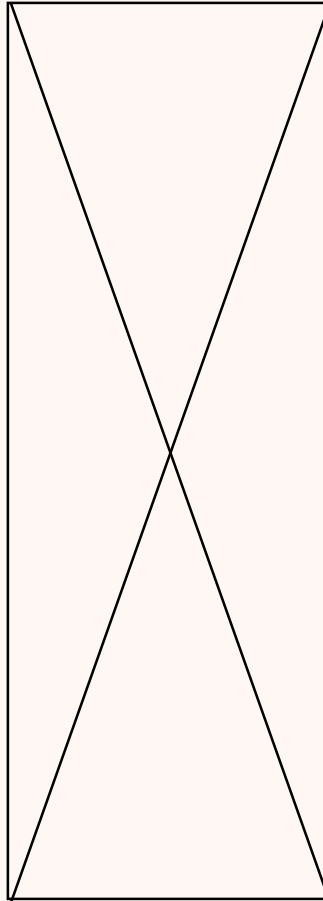
Model 3



Model 4



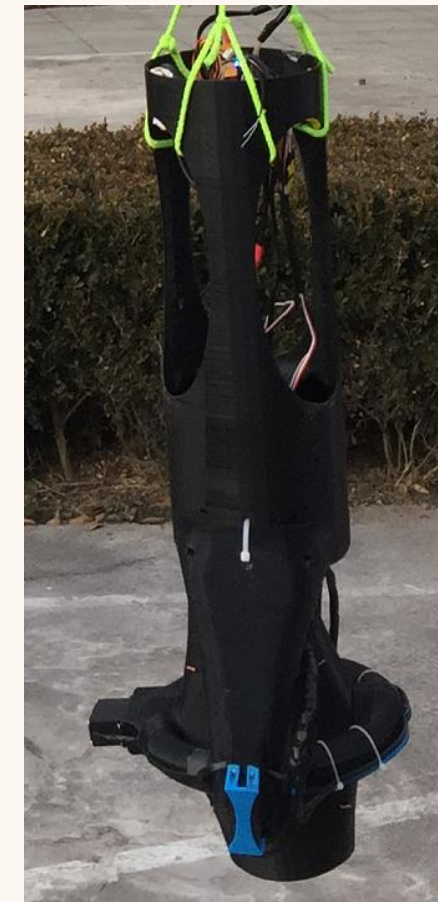
Model 1



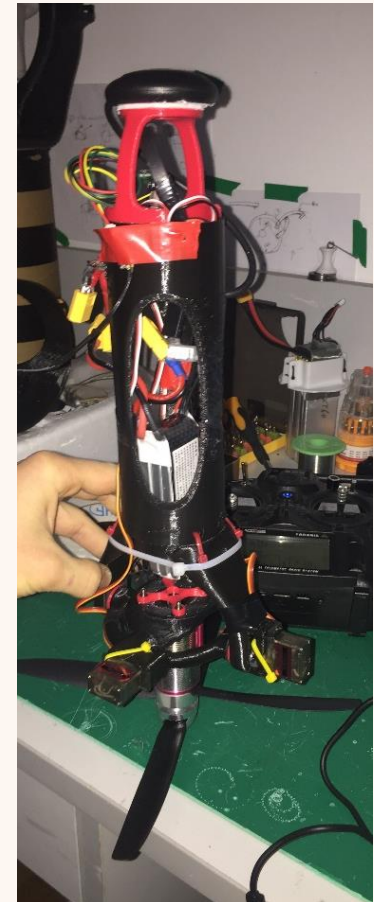
Model 2



Model 3



Model 4



- Engine system

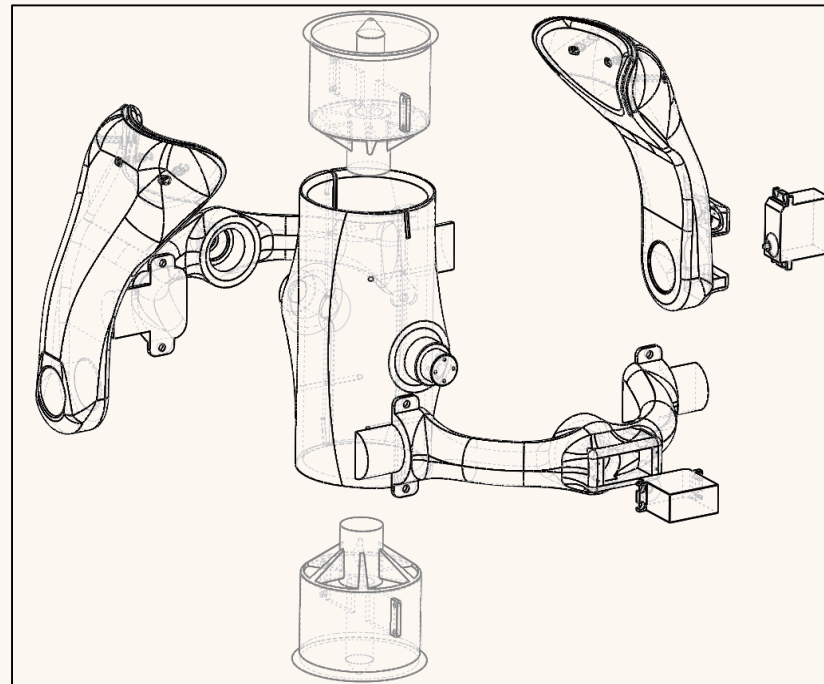


Fig. 59. Engine system N°1

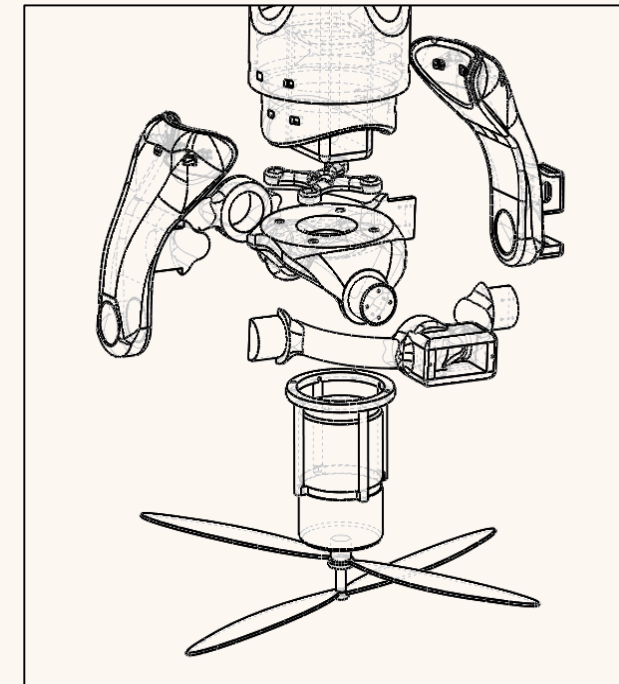


Fig. 60. Engine system N°2

- Ancillary equipment

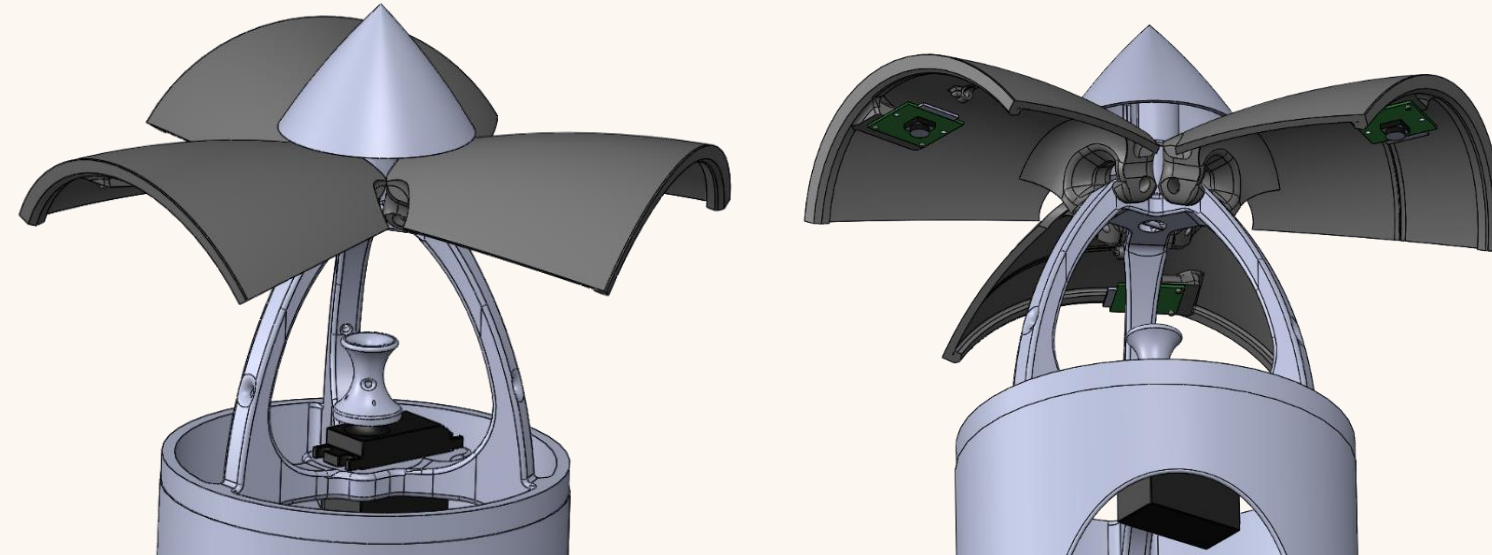


Fig. 61. Air brake and vision-controlled landing control camera

Design and Control for Reusable Booster of Launch Vehicle

BY

SIMON LE BERRE

UNDER THE SUPERVISION OF PROFESSOR

GONG CHUNLIN

MASTER OF FLIGHT VEHICLE DESIGN

XI'AN P. R. CHINA

JUNE 2020



Design and Control for Reusable Booster of Launch Vehicle

- Questions of reviewers

Q°1. Which specific RLV is studied in this work?

A°1

Q°2. What are the technical requirements?

A°2

A°2

Q°3. What is the expected assignment of this RLV?

A°3

Q°4. How explain the choice of the “Simple fin”, what mean the expression “linearity of control” ?

A°4

Q°5. How explain the reason to choose these four tops of the RLV during the global review of shape?

A°5

Q°6. Which parts of this Master thesis have been test by the real model?

A°6

Q°7. What is “6 Rotary idea to keep RLV balance “ ?

A°7

Design and Control for Reusable Booster of Launch Vehicle

BY

SIMON LE BERRE

UNDER THE SUPERVISION OF PROFESSOR

GONG CHUNLIN

MASTER OF FLIGHT VEHICLE DESIGN

XI'AN P. R. CHINA

JUNE 2020



Design and Control for Reusable Booster of Launch Vehicle

- Mathematic point N°1

Relationship between Y and Z Forces and Aerodynamic Forces (Lift and Drag).
By application of a 2D base change matrix.

$$P_{RLV,Velocity} = \begin{pmatrix} \cos(\alpha) & \sin(\alpha) \\ -\sin(\alpha) & \cos(\alpha) \end{pmatrix} \quad (1)$$

$$\begin{pmatrix} Drag_{force} \\ Lift_{force} \end{pmatrix} = P_{RLV,Velocity} \begin{pmatrix} Force\ Y \\ Force\ Z \end{pmatrix} \quad (2)$$

Ainsi:

$$Drag_{force} = F_y * \cos(\alpha) + F_z * \sin(\alpha) \quad (3)$$

$$Lift_{force} = -F_y * \sin(\alpha) + F_z * \cos(\alpha) \quad (4)$$

- Mathematic point N°2

$$a = n * \tan(pitch) \quad (18)$$

$$b = n * \tan(roll) \quad (19)$$

$$c = \sqrt{a^2 + b^2} \quad (20)$$

$$\alpha = \arctan(c/n) \quad (21)$$

$$\alpha = \arctan\left(\frac{1}{n} * \sqrt{n^2 \cdot \tan^2(pitch) + n^2 \cdot \tan^2(roll)}\right) \quad (22)$$

$$\alpha = \arctan(\sqrt{\tan^2(pitch) + \tan^2(roll)}) \quad (23)$$

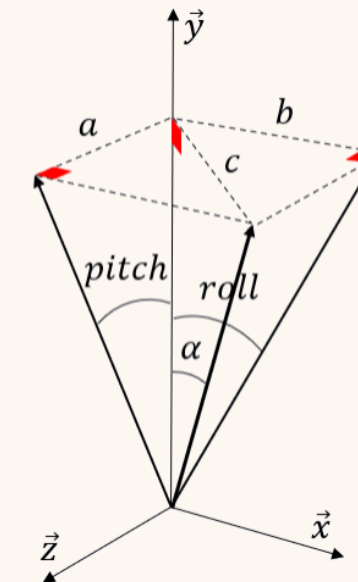


Fig. 28. 3D representation of the angle of attack

Design and Control for Reusable Booster of Launch Vehicle

BY

SIMON LE BERRE

UNDER THE SUPERVISION OF PROFESSOR

GONG CHUNLIN

MASTER OF FLIGHT VEHICLE DESIGN

XI'AN P. R. CHINA

JUNE 2020

Design and Control for Reusable Booster of Launch Vehicle

Q°1

- Which specific RLV is studied in this work?



Fig. 62. Space shuttle during take-off phase



Fig. 63. Falcon 9 during take-off phase

- Which specific RLV is studied in this work?

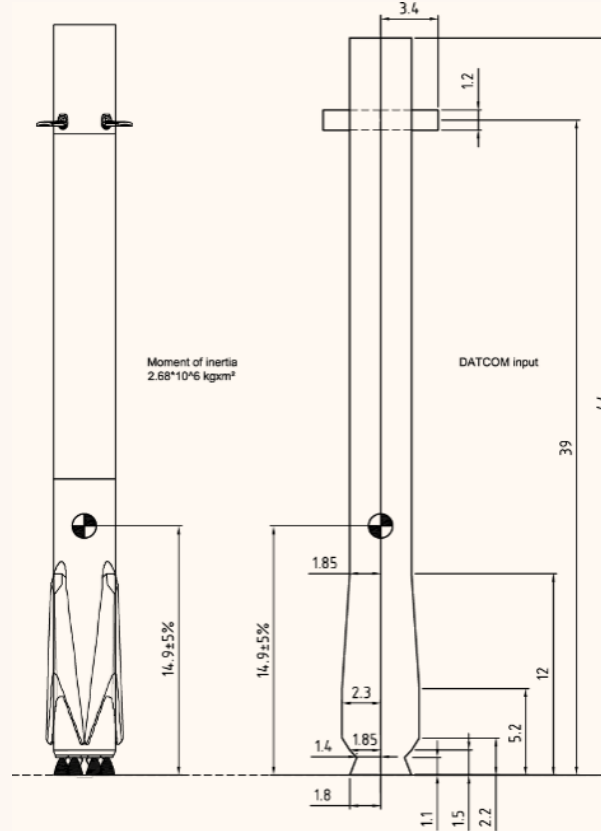


Fig. 64. Falcon 9 dimensions

Design and Control for Reusable Booster of Launch Vehicle

Q°3

- What is the expected assignment of this RLV?



Fig. 65. Ariane 5 during take-off phase



Fig. 66. SpaceX 's Star ship project

- Rotary idea to keep RLV balance

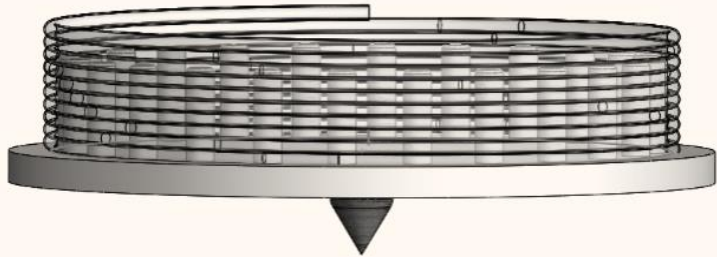


Fig. 67. Water Spinning top 3D model



Fig. 68. Water Spinning top and water pressure device

Design and Control for Reusable Booster of Launch Vehicle

BY

SIMON LE BERRE

UNDER THE SUPERVISION OF PROFESSOR

GONG CHUNLIN

MASTER OF FLIGHT VEHICLE DESIGN

XI'AN P. R. CHINA

JUNE 2020